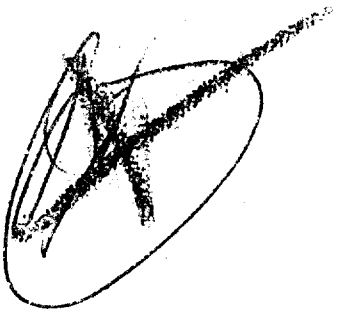

Epitaxial Vapor Growth of $Hg_{1-x}Cd_xTe$ in an Open-Tube Apparatus

70-M46-03

Epitaxial Vapor Growth of $Hg_{1-x}Cd_xTe$ in an Open Tube Apparatus

Final Report
(February 1969 to February 1971)

March 1970

by

D. R. Carpenter
A. T. Halpin
R. M. Kloepper
P. B. Pickar

Prepared under Contract N00019-69-C-0398

for

Naval Air Systems Command
Department of the Navy
Washington, D.C.

by

International Business Machines Corporation
Federal Systems Division
Electronics Systems Center
Owego, New York 13827

Table of Contents

List of Illustrations

List of Tables

FOREWORD

This investigation is a continuation of a former study of the epitaxial vapor growth of $Hg_xCd_{1-x}Te$, conducted under Contract N00019-68-C-0181. The objective is to understand and control the growth process such that material of specified composition and semiconductor properties may be synthesized. Data gathered prior to the present effort enabled the presentation of a model representing the qualitative growth mechanism. Using this model as a basis, the present study attempts to optimize the technique and apparatus for growth. Various analytical measurements have been performed on epitaxially deposited layers in an effort to relate material properties with conditions and mechanisms of growth. Further, photoconductive devices have been fabricated from the epitaxial $Hg_xCd_{1-x}Te$ layers. These devices have been used to collect data and catalog information on the effect of growth conditions on the resulting material properties.

The present program includes a considerable effort to gather more quantitative information on the functioning of the growth apparatus. Studies were initiated to measure the exact concentration of the reactant elements in the gas phase over the growing crystal by means of measuring the optical absorption of set wavelengths of light of the constituent elements just ahead of the reaction chamber. A second complete growth apparatus was designed and constructed to accomplish these optical density measurements.

Section 1

OPTICAL DENSITY MEASUREMENTS

Throughout the year, two crystal growing systems were in operation. One of the systems was operated under appropriate temperature conditions for desired crystal growth. The second system employed a more accurate and direct method for controlling the concentration of the constituents in the vapor mixture flowing into the growth zone. This method involves measuring the optical density of the individual source material being moved toward the reaction, or growth zone of the apparatus. Any of these concentrations can be adjusted by changing source temperature and/or the rate of carrier gas flow through the source zones.

The basis of this control approach is Beer's law of absorption, which can be expressed as

$$I = I_o \, 10^{-ncL}$$

where I is the intensity of transmitted light passing through a sample of thickness L
c is the concentration of absorbing substance (mole/liter)
n is the molar extinction coefficient of the absorbant at a given wavelength

Rewriting this expression in terms of optical density, we get

$$\log \frac{I_o}{I} = ncL = D \text{ (optical density)}.$$

The optical density which a vapor exhibits can be related to its partial pressure (p) empirically. A typical linear relationship would be exemplified by

$$p(atm) = kDL^{-1}$$

where the proportionality constant k is determined experimentally.

Calibration runs were carried out on static cells containing the vapors of the individual charges. Relationships between partial pressure, measured optical densities, and source temperatures were determined for a given set of cell dimensions, absorption wavelengths, and pressures for mercury, tellurium and cadmium.

1.1 EXPERIMENTAL TECHNIQUE (STATIC CELL)

The equipment used in these experiments includes a Perkin-Elmer Grating Spectrophotometer, Model 16U, a Bausch and Lomb Grating

(1200 lines/mm), an EMI Photomultiplier, Model 9592B, a hydrogen light source, and a Corning Glass Filter, CS7-54.

Optical densities of vapors of Hg, Cd, and Te were separately measured in individual closed static cells. All three cells were constructed from 20 mm OD quartz and were designed to present a 50 mm optical path length between a pair of flat, parallel quartz windows at each end. The cell temperature was maintained at 780°C by a resistance-wire furnace wound on the cell.

Every cell contained a quartz extension leg for attachment to a vacuum station, and which contained two charge sites (see Figure 1-1). The individual element was loaded into the charge site (B) farther from the optical cell within the static cell. Then the cell was heated to 750°C and outgassed at 1×10^{-5} torr for 6 hours. After cooling to room temperature but while still under vacuum, the charge was shifted to site (A) in the extension leg closer to the optical cell and brought up to the melting point. The cell was then sealed off at 1×10^{-5} Torr and the charge was again allowed to cool.

The zero point for optical density was then obtained with the optical cell at 780°C and the charge at or near room temperature. Subsequently, absorption data were taken as the charge, which was independently heated, was brought through a range of temperatures.

1.2 RESULTS

1.2.1 CADMIUM

Absorption peaks were found for cadmium at 3260 and 3340 A°. Because the latter measure was the more sensitive of the two, the optical density data were taken at that wavelength and plotted logarithmically (log D_{3340}) as a function of $10^3/T$, where D is the density and T is temperature in °K. This plot produced a straight line of slope -5.62×10^3/°K (Figure 1-2). In the temperature range from 316°C to 727°C, the vapor pressure, p, of Cd(g), as taken from the literature, follows the relationship

$$\log p_{Cd}(\text{atm}) = -5.30 \times 10^3/T + 5.106.$$

Noting that the slope of the measured data of Figure 1-2 agrees to within 6 percent of the literature value, one can say that Beer's law is obeyed reasonably well at 3340 A°, within the pressure range of 1.3×10^{-2} to 1.1×10^{-1} atm.

Figure 1-3 shows the relationship between Cd vapor pressure and its measured optical density. This is given as

$$p_{Cd}(\text{atm}) = \frac{27.2}{L} D_{3340}$$

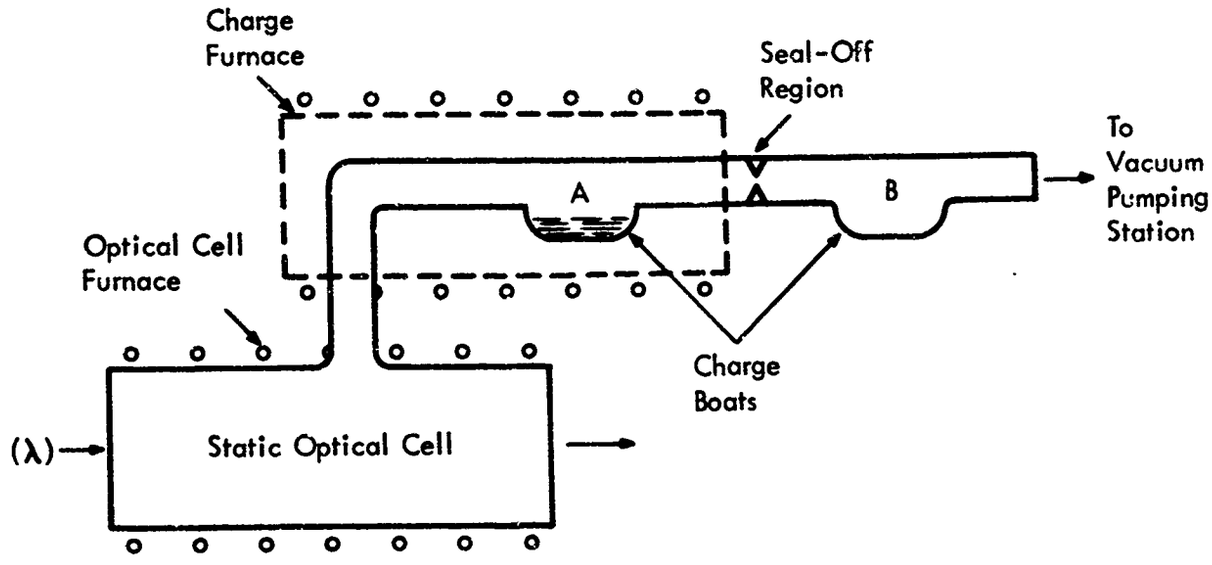

Figure 1-1
Static Cell

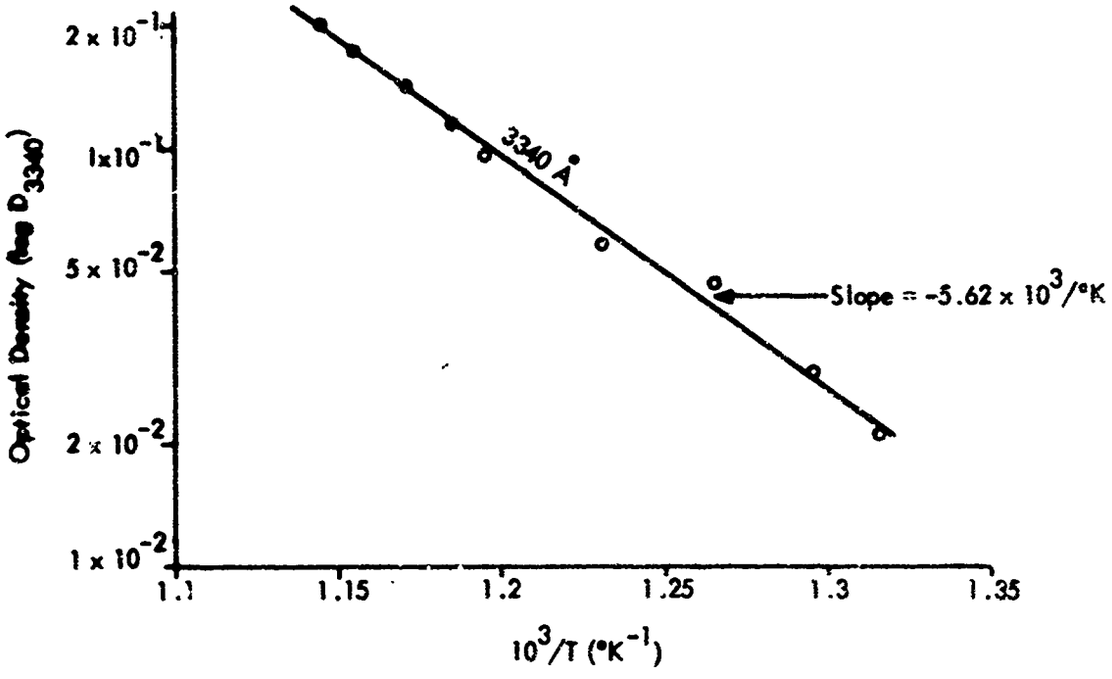

Figure 1-2. Optical Density as a Function of Cadmium Source Temperature

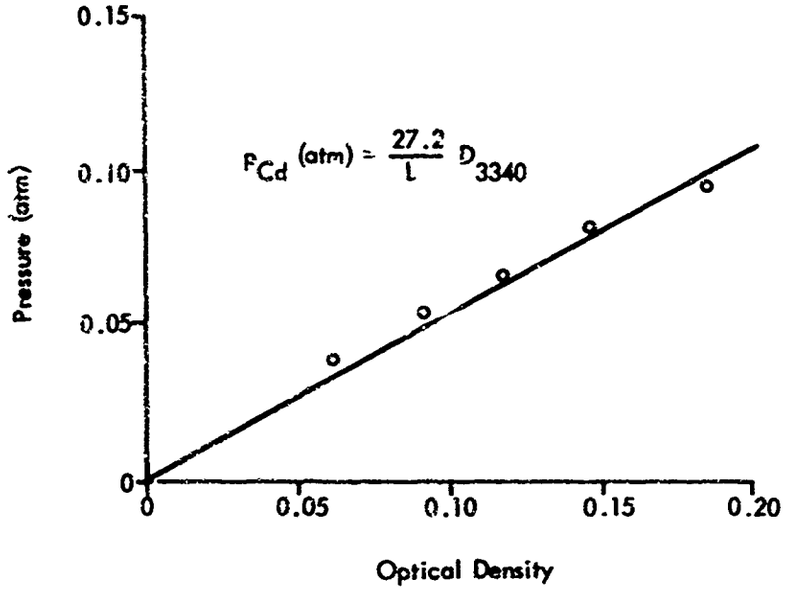

Figure 1-3. Cadmium Vapor Pressure as a Function of Optical Density

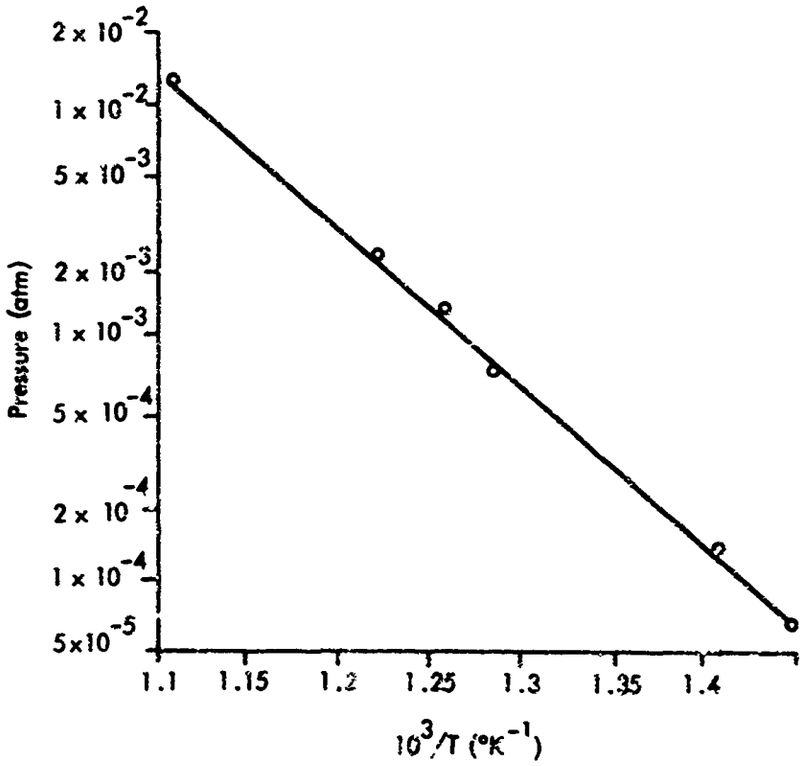

Figure 1-4. Tellurium Vapor Pressure as a Function of Source Temperature

where L is the optical path length in the vapor stream.

1.2.2 TELLURIUM

An absorption peak for $Te_2(g)$ was located at 2715 A° for a hydrogen lamp radiation source. Previous $Te_2(g)$ absorption data at 4357 A° for a tungsten lamp are also included in this section.

In Figure 1-4, Te_2 vapor pressure data plotted as a function of 1/T°K yield the following equation:

$$\log p_{Te_2}(atm) = -6.57 \times 10^3/T + 5.3$$

This straight-line plot has a slope of -6.57×10^3. The measured optical density plotted as a function of temperature (1/T) yields straight-line relationships (Figure 1-5) having slopes within 5.6 percent of the values obtained for the pressure-temperature case. Therefore, within the pressure and temperature ranges indicated below, Beer's law is reasonably followed at the two wavelengths:

Wavelength (A°)	Slope m ($\times 10^3$)	Δm (% error)	p (atm $\times 10^{-2}$)	T (°C)
2715	-6.4	5.6	0.1 - 1.3	512 - 520
4357	-6.9	5.0	0.02 - 4	573 - 457

As shown in Figure 1-6, we obtained the following calibration relationships:

$$p_{Te_2}(atm) = \frac{0.237}{L} D_{4357}$$

$$p_{Te_2}(atm) = \frac{1.25}{L} D_{2715}$$

1.2.3 MERCURY

The pressure-optical density relationship as found for Te_2, and Cd was also found for Hg: namely, at wavelength $\lambda = 2700$ A°, pressure (atm) = $32.6 (D_{2700}/L)^{1/2}$.

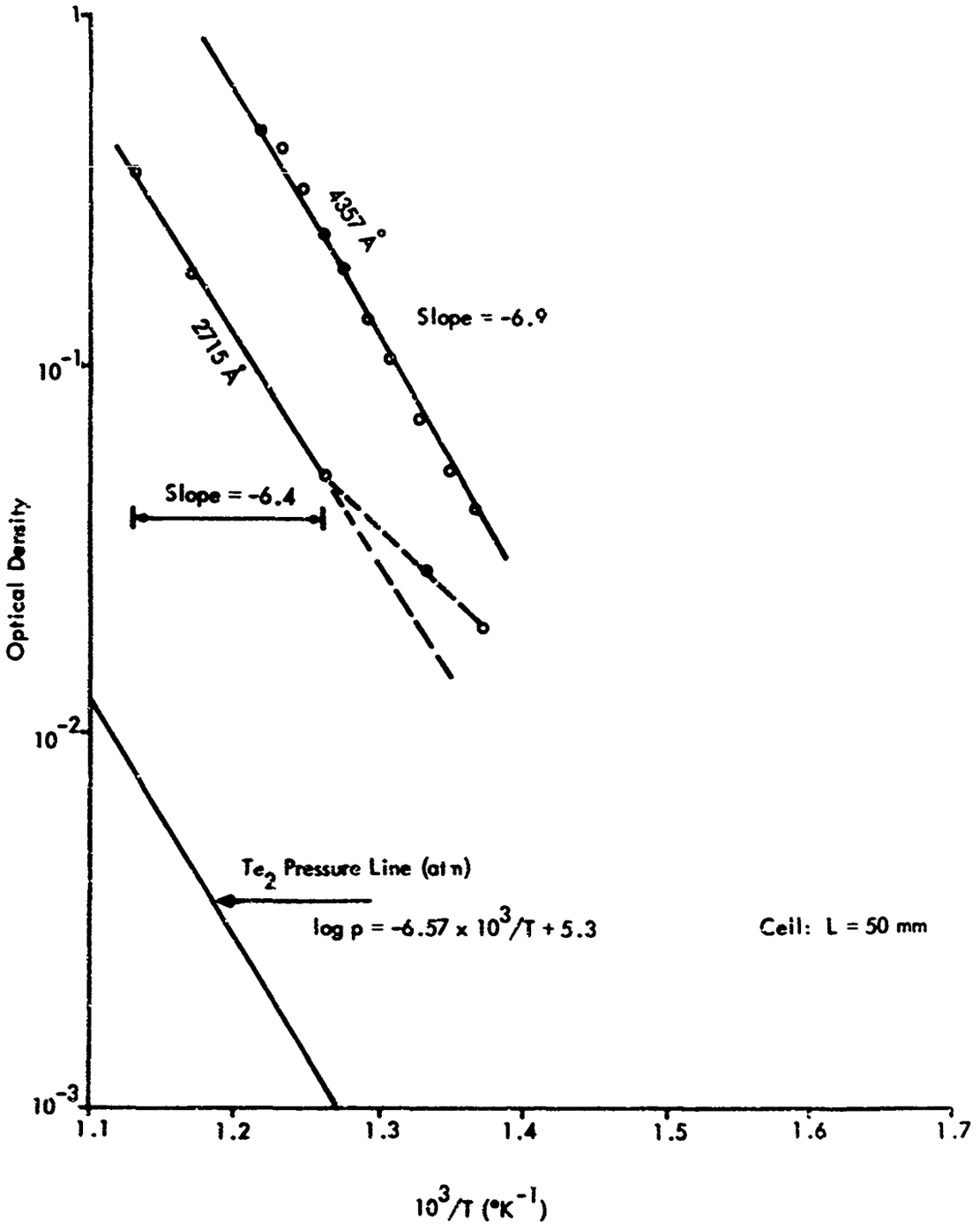

Figure 1-5. Optical Density as a Function of Tellurium Source Temperature

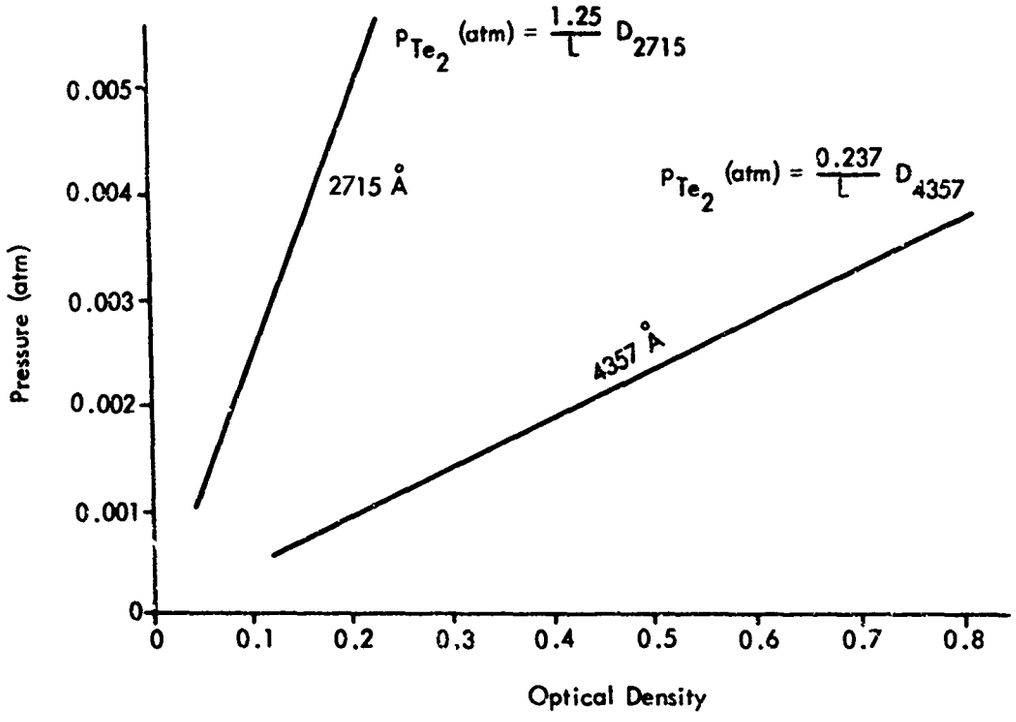

Figure 1-6. Tellurium Vapor Pressure as a Function of Optical Density

Section 2

OPTICAL DENSITY MEASUREMENTS

2.1 DYNAMIC FLOW SYSTEM

After establishing the experimental fact that Beer's law of absorption is obeyed for the appropriate wavelengths for each of the constituent material in the static cells, the application of this law for the open-tube technique was then studied. Experiments were then performed using the entire open tube growth system.

The vapors of mercury, cadmium, and telluride (with a carrier gas) were flowed through this system and the results compared with data obtained in static systems. Variances in the relationships between optical density, vapor pressure, and source temperature have been noted. This was expected since the "steady state" condition of a closed static cell can be acheived in a dynamic flow system only under specific operating conditions. This area of study is currently underway and the following describes results obtained with individual vapors. In general, the data indicates that under specific operating conditions one can indeed obtain the same relationship between optical density and source temperature as in a closed system.

2.2 EXPERIMENTAL

A second open-tube growth apparatus was constructed which included a heated optical cell for density measurements. The cell was located downstream in the mixing furnace just ahead of the growth furnace. Thus, all three metallic vapors, plus the carrier gas, must necessarily pass through the optical cell prior to entering the deposition zone.

The optical cell consists of a quartz tube, 21 mm OD, bounded on each end with a pair of spaced quartz windows. Temperature is monitored internally by a chromel-alumel thermocouple located in a quartz well inserted into the side of the cell. Furnace windings are extended beyond the viewing windows to prevent condensation on these ports. The optical path length was 90 mm.

Upstream the three sources were located in separate furnaces. Carrier gas (research grade forming gas) was flowed into the system at one end of each of the three source furnaces. The vapors were allowed to pass into a mixing zone just upstream from the optical cell where the temperature was maintained at 750°C to prevent reaction of the co-existing vapors.

Optical density measurements on the individual flowing metallic vapors plus carrier gas have been performed. These data do not include binary or ternary combinations as yet.

Wavelengths at which absorption data were measured are 2600 A° (mercury), 3261 A° (cadmium), and 4357 A° (tellurium). Optical density measurements were obtained using a Perkin-Elmer Model 16U Grating Spectrophotometer.

2.3 RESULTS

2.3.1 MERCURY

Figure 2-1 depicts a plot of log D (optical density) as a function of source temperature. Two regions are discerned having distinctly different slopes (d log D/d (1/T)). At lower Hg source temperatures (higher 1/T values) one sees that within a given run, the slope is substantially in agreement with that predicted from static cell data. This shows that as the source furnace temperature is raised, the vapor overpressure in the open tube apparatus is following the static relationship

$$\log p_{Hg}(atm) = -3.08\ (10^3)/T + C$$

where C is a constant ($\log p_o$).

It is also evident that the resultant optical density varies with $(p_{Hg})^2$ and that Beer's absorption law is applicable in this temperature and pressure range.

At 359°C, the vapor pressure of mercury reaches one atmosphere. Our open tube system obviously cannot support pressures exceeding 1 atm so that for source temperatures greater than 359°C, Hg vapor moves out of the system at a rate sufficient to satisfy the 1 atmosphere limit.

In these runs, both mercury vapor and a carrier gas were employed. Since the sum of the partial pressures of carrier and mercury must not significantly exceed one atmosphere, we can assume that for ever-increasing source temperature, mercury vapor pressure p(Hg) will approach 1 atmosphere asymptotically. As a consequence, optical density values which reflect p(Hg) will assume such a relationship with temperature. This is illustrated graphically in Figure 2-1 where D(Hg) at increasing temperature is approaching the maximum value expected for one atmosphere of p(Hg).

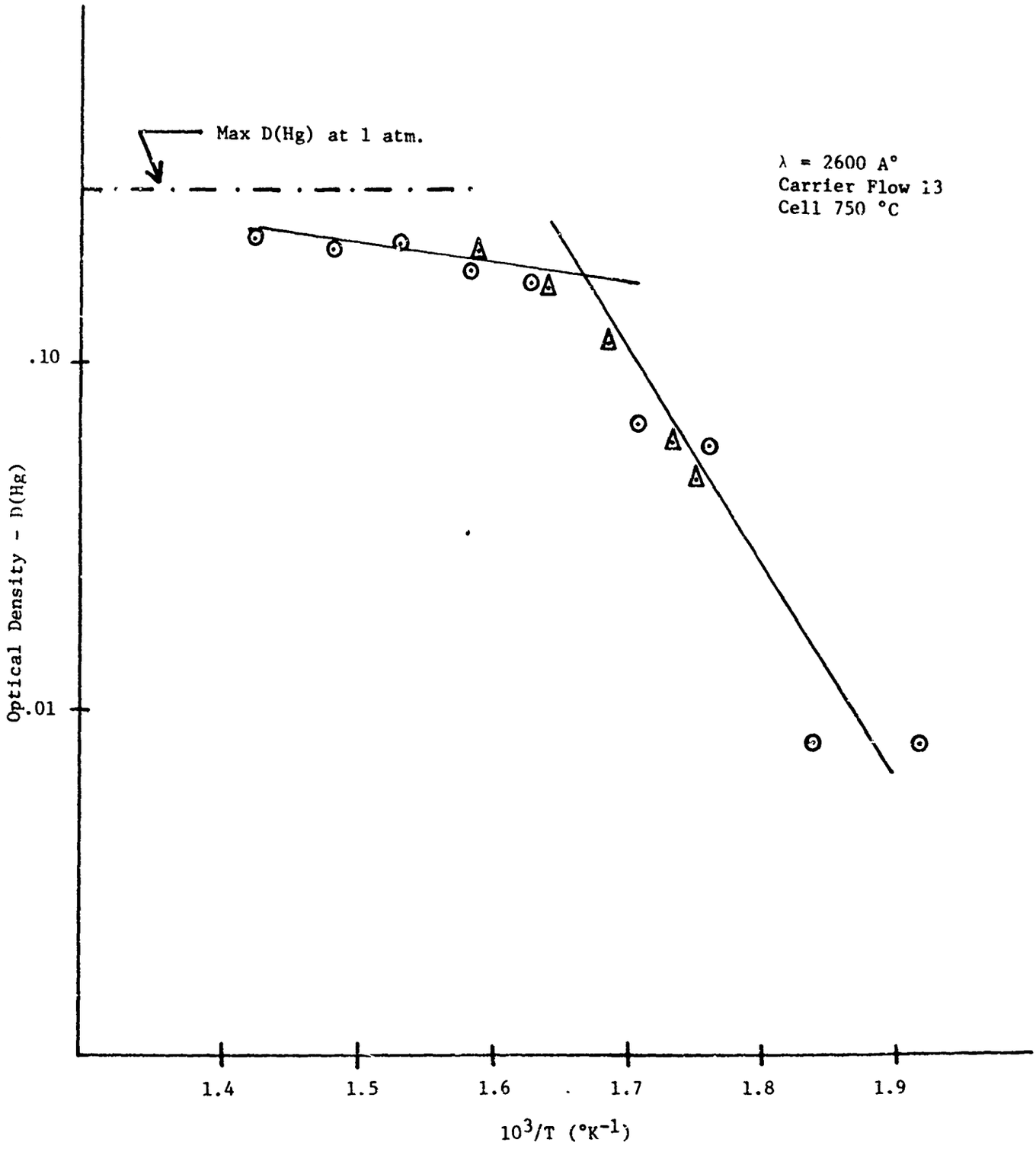

Figure 2-1
Optical Density (Hg) vs. $10^3/T$

2.3.2 TELLURIUM

Figure 2-2 illustrates a typical plot of the relationship between measured optical density of Te_2 vapor and source temperature. Note that the straight line slope of the curve in the open tube system (with carrier gas flow) and that obtained for closed static cells are in general agreement. This indicates that 2) partial pressure - temperature equilibrium is achievable in the dynamic system; and b) Beer's absorption law is being followed. That is, the relationship between partial pressure and optical density established for Te_2 in a static cell applies as well under the dynamic conditions employed here.

2.3.3 CADMIUM

Absorption data were obtained for cadmium vapor at 3261 A° over the temperature range 590°C - 425°C. The resultant data plotted as optical density vs. temperature (Figure 2-3) for this dynamic system did not follow the form predicted by static cell measurements. Whereas the latter yields a slope of -5.3 for log D vs. 1/T, the former yields shallower slopes.

Subsequent tests showed the presence of a small leak in the quartz dynamic system in the Cd source furnace. This resulted in substantial oxidation of the Cd source which was beyond the reducing capacity of the carrier gas hydrogen component. Repairs are being effected on the system now. Also, a forepump and vacuum thermocouple are being installed to enable us to monitor the tightness of the growth apparatus. When we resume Cd runs, we would expect similar results as in the Te_2 case since both species are examined over a comparable range and magnitude of pressures.

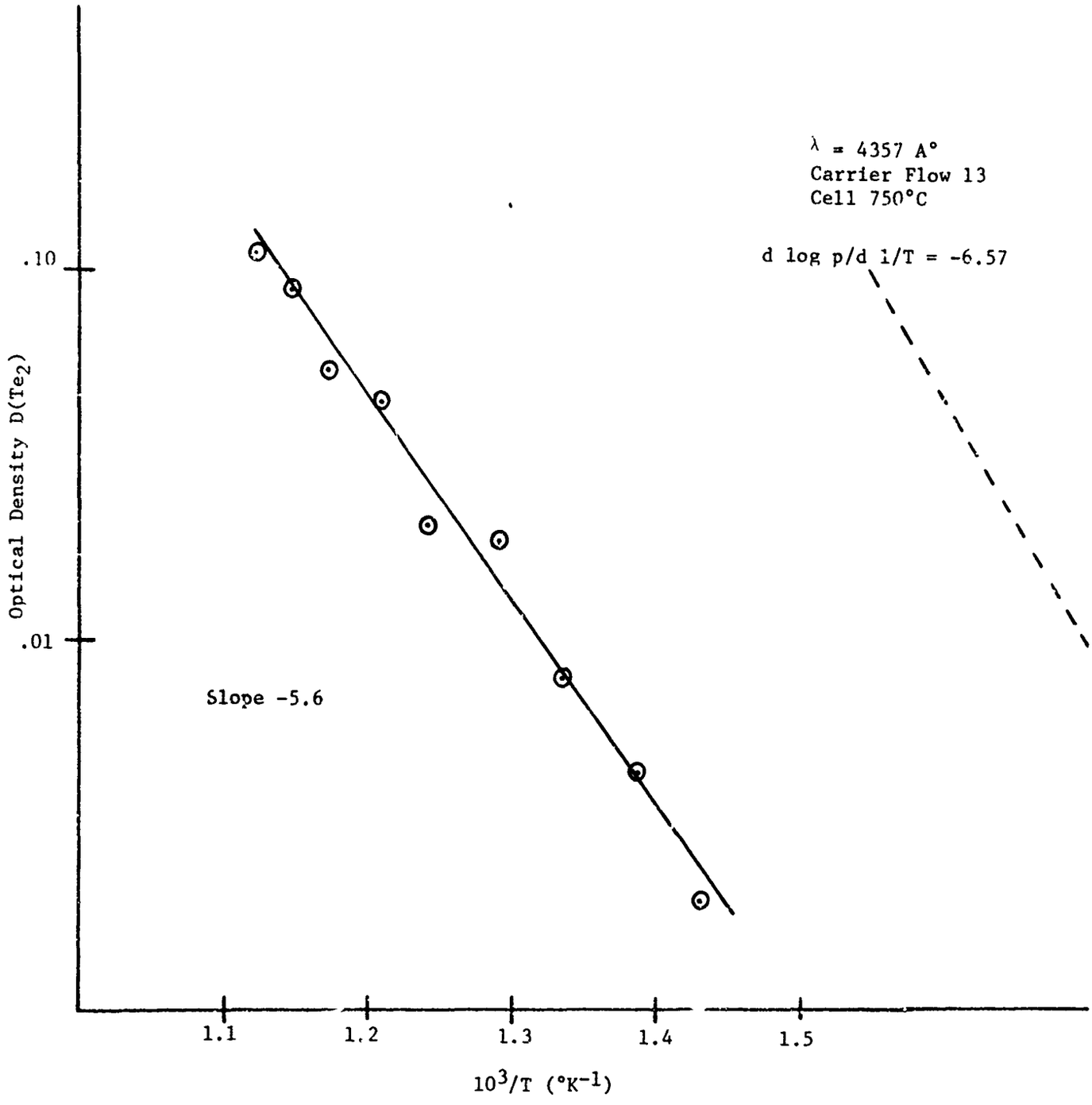

Figure 2-2
Optical Density (Te_2) vs. $10^3/T$

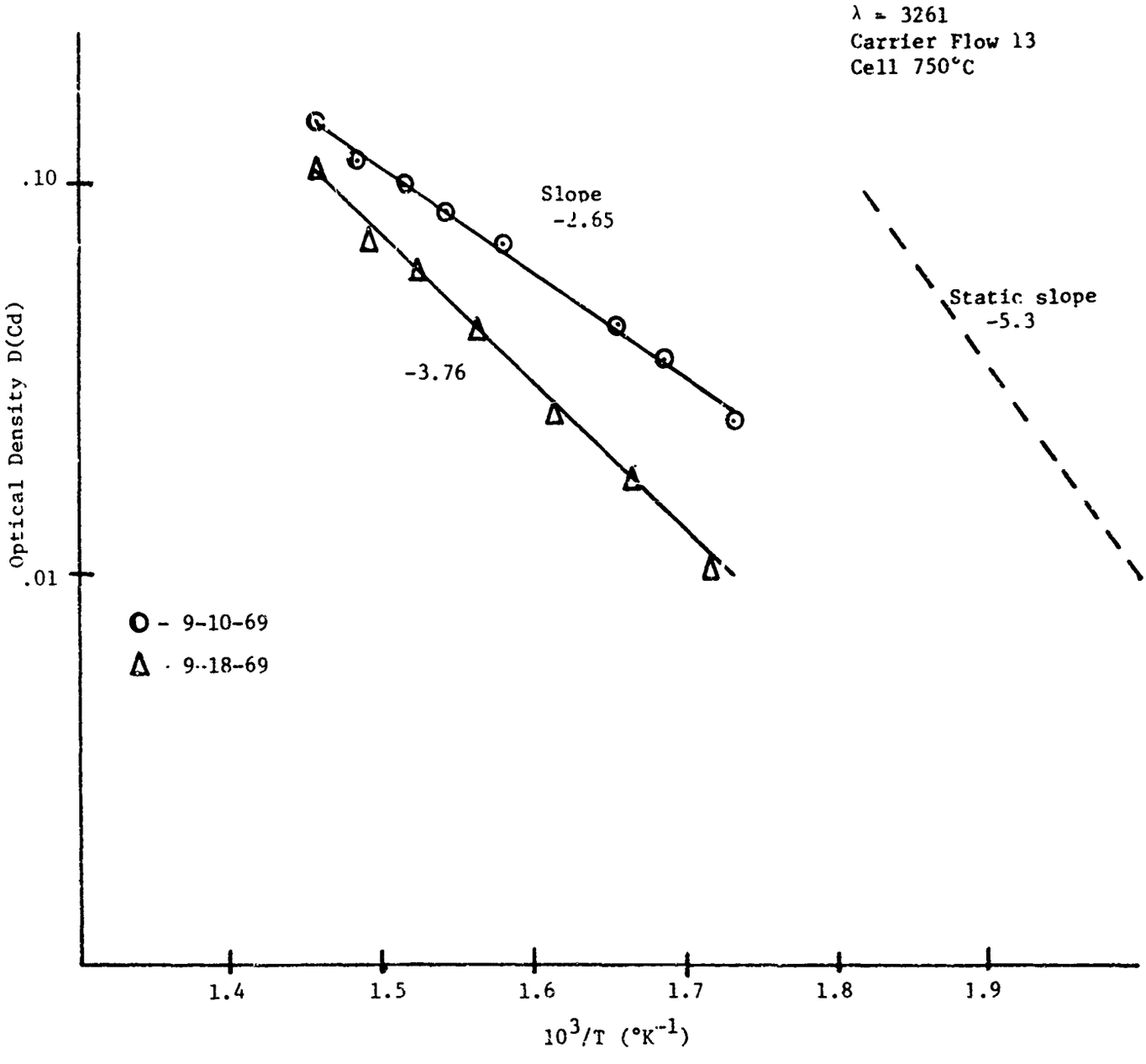

Figure 2-3
Optical Density (Cd) vs. $10^3/T$

Section 3

EQUIPMENT IMPROVEMENTS

3.1 SUBSTRATE TEMPERATURE CONTROL

In addition to the precise temperature control which one must exercise over the temperature on the source furnace, premix furnace and growing chamber, in order to provide the proper partial pressures and mass transported to the substrate, the temperature control of the substrate holder is also of utmost importance. During the period in which the open tube system evolved, the pedestal which contained the substrate holder was fabricated from quartz. The substrate holder itself was a very thin disk of quartz attached to the pedestal. For cooling purposes, a jet of cool air was sprayed on the underside of the substrate holder. A thermocouple, encased in thin walled quartz, was placed in intimate contact with the substrate holder to monitor its temperature during the growth period. Because of the thermal conductivity of quartz, it was observed that a radial temperature gradient existed across the substrate holder. This gradient gave rise to a change in stoichiometry across the crystal surface.

In order to handle this problem, several techniques were studied. An obvious solution to the problem of having a uniform temperature on the substrate would be to incorporate the use of a heat-pipe into the cold finger. However, because of the temperature involved, several heat-pipe vendors did not respond to the specification sent them: consequently, it was assumed that a heat-pipe for this system was not available.

Another technique proposed and now settled on is the balanced-heat radiation method. The equipment fabricated for this purpose is shown in Figure 3-1. The material from which this device is made is tantalum, since it can be employed at high temperature, with little or no reaction to most elements.

In actual practice, the substrate and its holder sees the temperature of its surrounding environment, which is 750°C. This temperature is too high for crystal growth. It must be reduced substantially to about 600°C. To accomplish this end, a cool working gas from a heat exchanger is passed up through the center tube of the device. This cooling gas impinges on the bottom of the substrate holder after passing through a gas diffuser and an electric heating element. The temperature of the working gas is so controlled that it cools the substrate to, say, 550°C, which is too low for

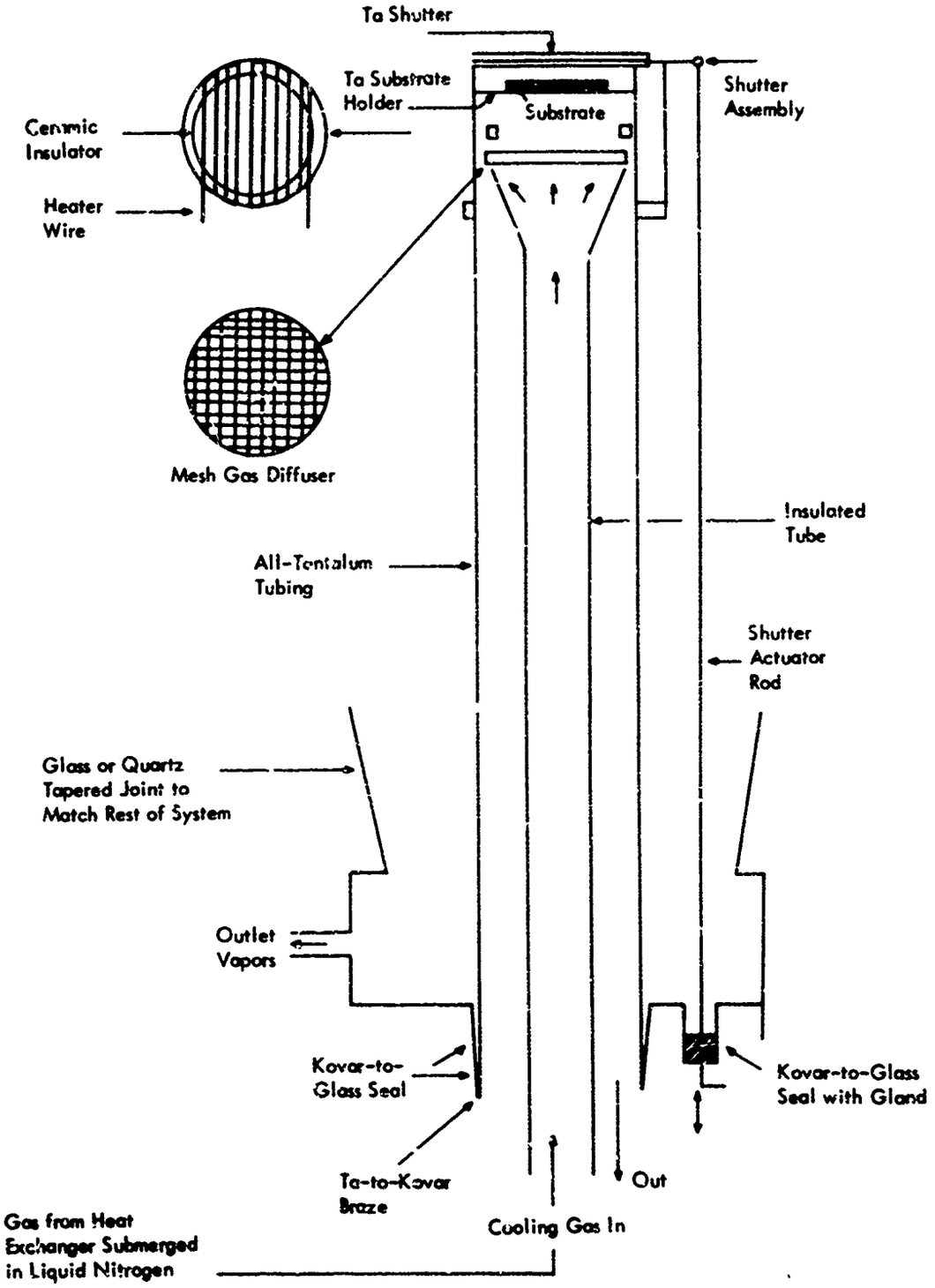

Figure 3-1. Balanced-Radiation Apparatus

growth. At t' , point, the electronic .ontroller connected to the internal hea' . takes over to supply a sufficient amount of energy to raise the substrate to a constant temperature of 600°C. The temperature of the substrate holder is monitored and controlled by four thermocouples attached intimately to it. In simulated crystal growing experiments, this device exhibits a very small radial temperature gradient.

Section 4

ELECTRICAL MEASUREMENTS

4.1 HALL MEASUREMENTS

The method involved in making DC Hall effect and resistivity measurements are well described in the literature. The measurements are carried out by placing the specimen in a vacuum chamber which allows control of the temperature of the sample and the atmosphere surrounding it. In these experiments, room temperature measurements are carried out in a vacuum. Liquid nitrogen temperature measurements are made by placing the vacuum probe in a dewar containing liquid nitrogen. The temperature is monitored by a thermocouple placed adjacent to the sample.

The measuring instruments used in this work are a Leeds and Northrup six-dial potentiometer, Model 7556, and an electronic dc null detector, Model 9834. The sample current is supplied by a well-regulated power supply. The current is determined by measuring the voltage drop across a standard resistor. A bucking voltage is also supplied to take care of IR drops across the legs of the sample.

The magnetic field is supplied by a Varian Model V-4004 electromagnet with the associated power supply, Model V-2300-A, and current regulator, Model V-2301-A. Measurements are normally made at magnetic field strengths of 5000 oersteds.

The precision in resistivity measurements is limited only by the stability of the circuits involved. In all cases, this can be made better than 1 percent. The precision in Hall effect values is limited either by stability of the measuring circuits or by the reproducibility of the magnetic field. Since the magnetic field is determined by setting the magnet current, hysteresis effects can lower the reproducibility of the magnetic field. However, with proper cycling of the magnetic field, this effect should be on the order of 1 percent or less. Thus, for the Hall coefficient, carrier concentration, resistivity, and mobility, it should be possible to obtain precisions on the order of less than 1 percent.

The absolute accuracy of the resistivity measurement in practically all cases is determined by the measurement of the distance between the resistivity probes. From measurements on the distance between the resistivity legs of the sample, this uncertainty has been determined to be on the order of about 5 percent.

The absolute accuracy of the Hall measurement is limited in most cases to the accuracy of the calibration of the magnetic field which should be good to 2 percent or better.

In general, then, the accuracy for Hall coefficient and carrier concentration determinations is about 2 percent. The accuracy for resistivity is about 5 percent, and thus the accuracy for mobility should be about 7 percent.

The equipment used for these experiments was checked by using standard samples of GaAs, calibrated by other laboratories.

The errors which occur, and the accuracy of the measurement, of course, also depend on the precision of the thickness measurements and the measurements of the physical dimensions of the specimens. These measurements were made by the use of a Reichert Zetopan Research Microscope.

Samples used for Hall measurements were six millimeters long and two millimeters wide. These samples had the customary two Hall legs on one side with another one on the opposite side. Some samples were grown through a stainless steel mask, while others were produced by a scribing technique. In all cases, they were essentially of the same size.

During this year, a considerable number of "as grown" samples were used for Hall measurements at room and liquid nitrogen temperatures. Typical results of these measurements are shown in Table 4-1.

Table 4-1
HALL MEASUREMENT DATA

	R(cm^3/coul)		μ(cm^2/v-sec)		(ohm-cm)		n(percm^3)		t film thickness in microns
Sample No.	Room	Liquid Nitrogen	Room	Liquid Nitrogen	Room	Liquid Nitrogen	Room	Liquid Nitrogen	
CK-87	-57	-121	5229	14,969	10×10^{-3}	9×10^{-3}	1×10^{17}	5×10^{16}	40
CK-90	-29	-122	2230	12,577	13×10^{-3}	10×10^{-3}	2×10^{17}	5×10^{16}	33
CK-91	-63	-142	4800	13,920	12×10^{-3}	12.7×10^{-3}	9.9×10^{16}	4.5×10^{16}	34
CK-91 after annealing at 1 1/2 atmos of Hg for 30 hours									
CK-91	-6.91	-7.6	3420	4222	2×10^{-3}	2.1×10^{-3}	7×10^{16}	6×10^{16}	34

Preliminary annealing measurements were begun during the latter part of this year. To accomplish this end, a quartz ampule was fabricated containing a well for containing the mercury. A sample was placed in the ampule and evacuated to 10^{-6} Torr at which time the ampule was sealed off. The ampule was placed in a temperature controlled furnace and the temperature was raised until 1 1/2 atmospheres of pressure was attained. The system was allowed to stay in this state for 30 hours.

Hall measurements on Sample CK-91 treated in this manner are seen in the above table (Table 4-1).

It was observed that the annealed samples show a definite dependence of both the carrier concentration and mobility on the annealing mercury pressure. This was observed in the limited number of samples thus far treated. The decrease in the Hall coefficient at high mercury pressures as observed in several different experiments is possibly due to increased donor concentrations.

The magnitude of the Hall coefficient appears to be a strong function of the mercury pressure; also, from the few experiments done thus far, it appears that the carrier concentration can be minimized by the correct mercury pressure during the annealing process.

Section 5

GROWTH STUDIES

5.1 GROWTH PARAMETERS VIA APL/360

All growth parameters and all data describing the detector results are now entered, via APL/360, in a data processing machine memory. The typical growth parameters which are contained for any series of growth runs include the following: run numbers, furnace temperatures (growth, mix, and pre-mix), source furnace temperatures (mercury, cadmium, and tellurium), air flow rate to the cold finger cooling pedestal, and cold finger temperature as a function of time. The analytical results which are contained in the data processing machine memory are: the X-ray fluorescence analysis of the percents of mercury, cadmium, and tellurium and the total counts from this analysis. The detector results which are entered into the data storage are stored for each detector evaluated (nine to ten detectors per growth run): sapphire cutoff, average sapphire cutoff for all detectors on the chip, resistance at both room temperature and liquid nitrogen temperature, the signal-to-noise ratio, the signal and bias at that maximum signal-to-noise ratio, the ratio of signal per bias and the signal at a given bias. These data are processed to attempt to correlate the growth parameters, the analytical results, and the detector results. Correlations may be tested against hypothetical functions or by plotting, using an automatic plotting routine, parameters against results. Many of these plots are included in Sections 5.2 and 5.3 of this report.

5.2 COLD FINGER

Normally, one thermocouple for controlling the temperature on the cold finger is used. However, to study any variation in crystal growth due to variations in temperature across the substrate, a second mobile thermocouple was employed. This second cold finger thermocouple had previously been added to the equipment, but its use as a control thermocouple has been discontinued. For six runs, the second thermocouple was monitored, after which its use was entirely discontinued; all controls of the cold finger pedestal temperature were made during this series of runs on the fixed thermocouple #1 in intimate contact with the top of the cold finger growth pedestal. Using thermocouple #2 as a temperature sensor with variable position, it was possible to map the temperature distribution on top of the cold finger growth pedestal. Figure 5-1 is a plot of the temperature as recorded by thermocouple #2 while thermocouple #1 was held at 600°C. The air required to maintain that 600° temperature is also plotted on this graph. The temperature distribution on top of two sapphire semicircles is demonstrated in the diagram of Figure 5-2, along with the corresponding air flow requirements; again, the temperature of thermocouple #1 was maintained at 600°C.

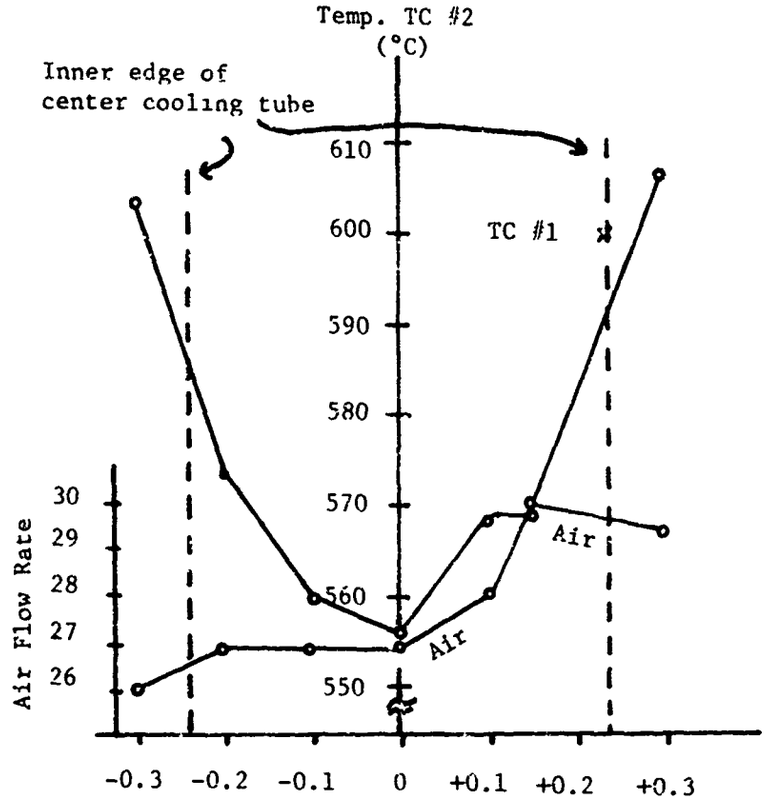

NOTE: TC #1 600°C

Figure 5-1
Cold Finger Temperature vs. Distance from Center

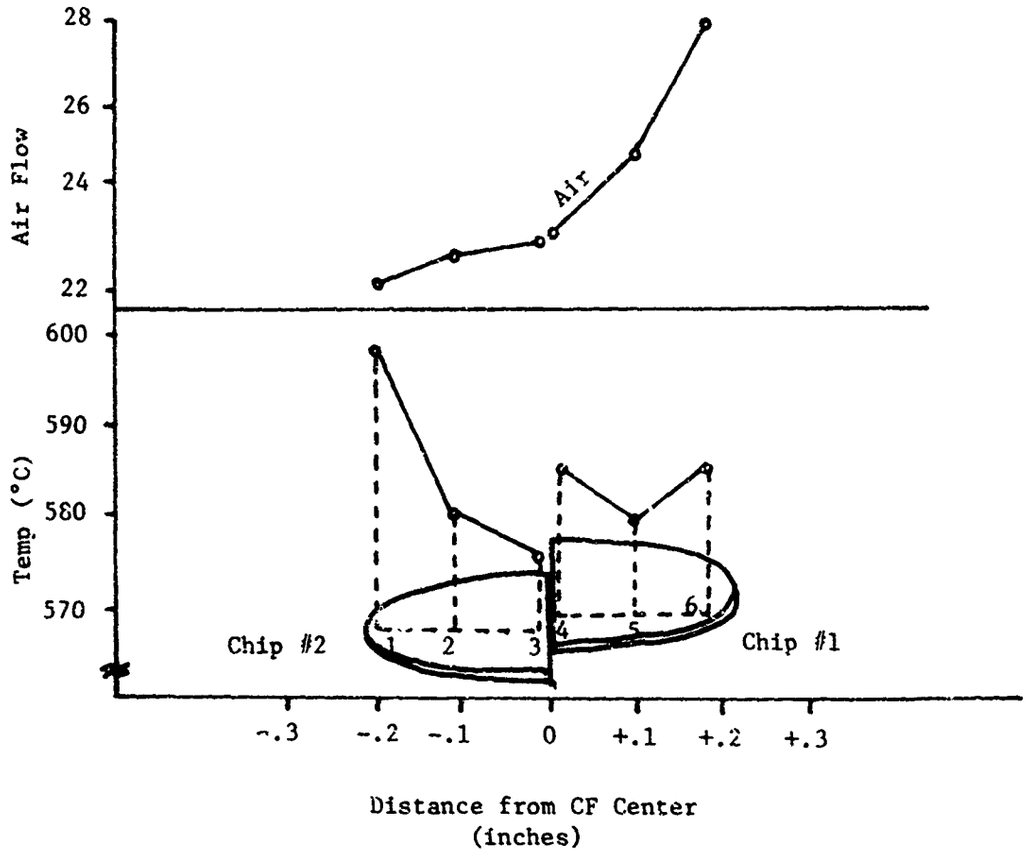

Figure 5-2
Temperature Distribution on Sapphire Substrates

5.3 GROWTH OF MATERIALS

In one set of experiments, of the 32 runs made, growths were made on 41 semicircles of sapphire, eight alumina substrates, eight groups of chips of cadmium telluride (semi-oriented), and two pieces of barium fluoride. Of these various materials, no cadmium telluride chips showed any success as detectors; one or more from each run were evaluated. The two growths on barium fluoride were produced for Hall measurements and have not yet been evaluated. Of the seven alumina substrates (one-quarter inch by one-half inch) two were not evaluated and only one of the remaining was classifiable as a (C) detector. For classification of detectors, see second quarterly report. Of 41 sapphire semicircles, 2 were not evaluated. The distribution of the various resulting classifications of the growths on sapphire, when evaluated as detectors, is shown in Table 5-1.

Table 5-1

EVALUATION OF DETECTORS

Class	Sapphire #	%
A	4	10
B	7	18
C	4	10
D	3	8
E	1	3
F	2	5
G	2	5
H	0	
I	0	
Not classified	16	41
Total	39	100

The results of the cold finger scan, using thermocouple #1 as the control, are shown in Figures 5-3A, 5-3B, and 5-3C. In these figures, the letter classification of the resulting detectors has been entered near the plotted points. In these experiments, it was observed that the best quality detectors (A's and B's) were produced at a cold finger temperature in the vicinity of 594° to 602°C with those overpressures of mercury, cadmium, and tellurium. The percent sapphire cutoff of the resulting detectors is illustrated in Figure 5-3C; although the sapphire cutoff remains relatively high (in the vicinity of 90 percent), as the cold finger temperature is lowered, the sensitivity of the resulting detectors decreased. In this optimum range, the percent mercury,

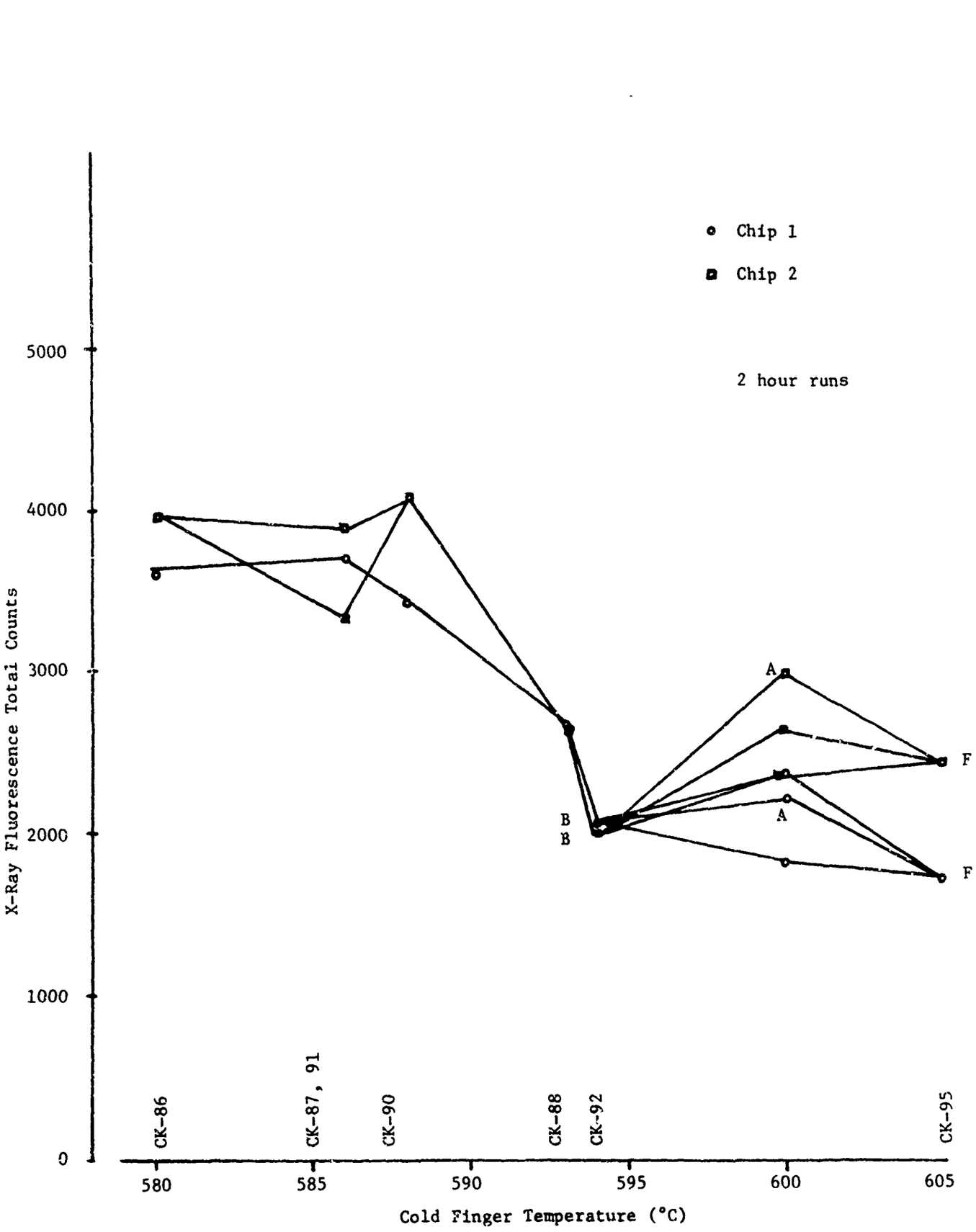

Figure 5-3A
X-Ray Fluorescence Total Counts vs. Cold Finger Temperature

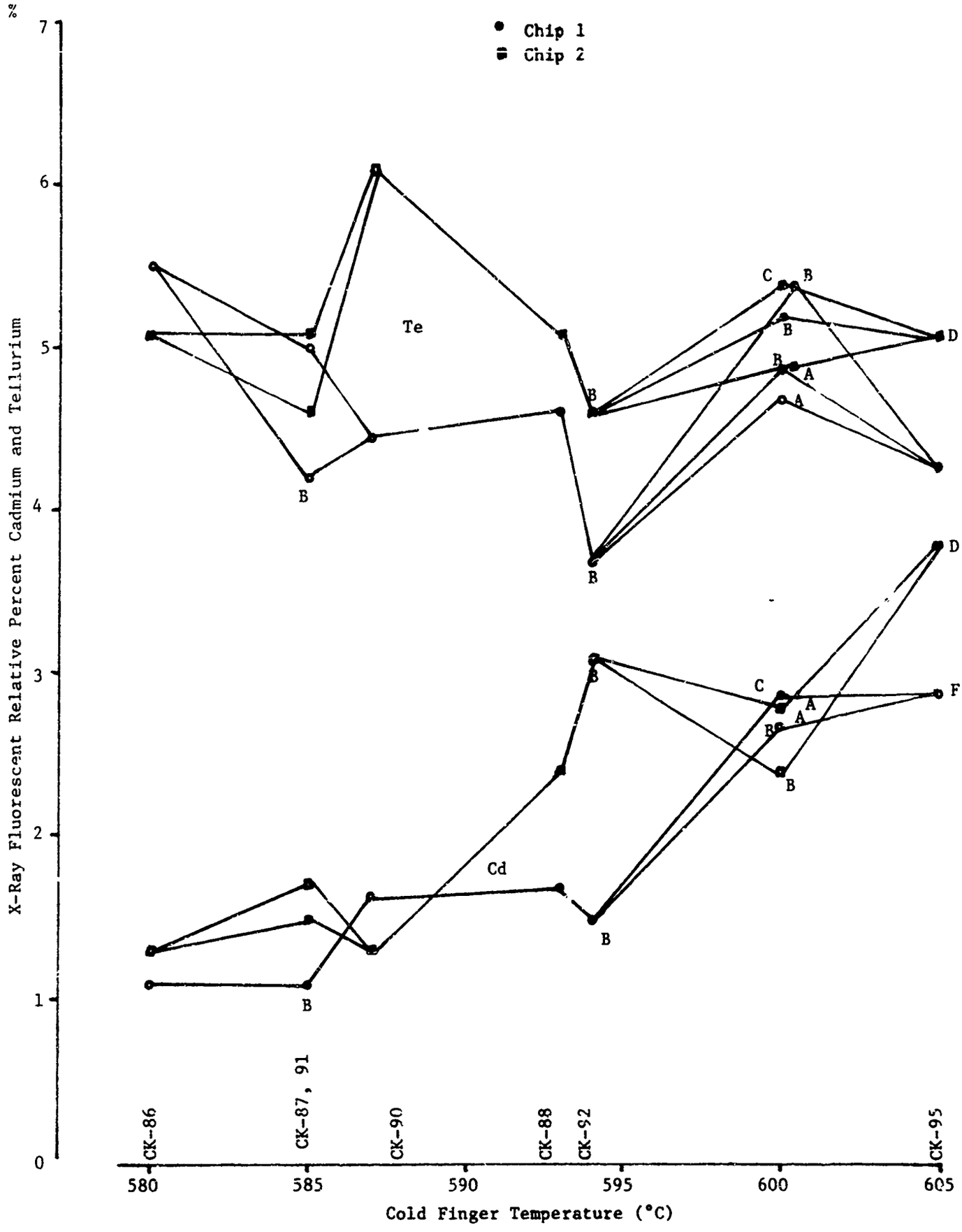

Figure 5-3B
Relative Percent Cadmium and Tellurium vs. Cold Finger Temperature

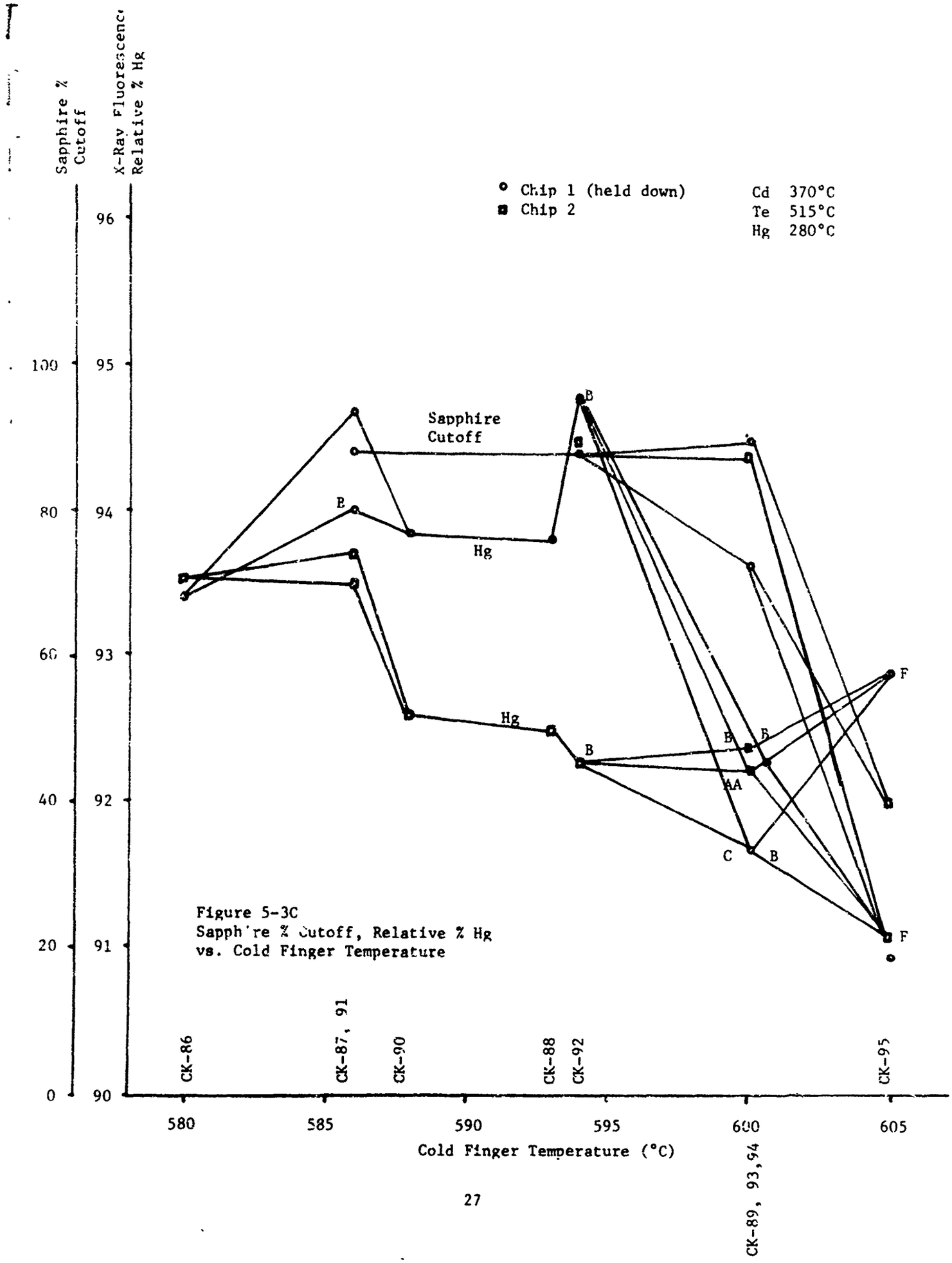

Figure 5-3C
Sapphire % Cutoff, Relative % Hg
vs. Cold Finger Temperature

cadmium, and tellurium content as measured by the relative x-ray fluorescence counts are 92 percent, 2 to 3 percent, and 4 to 5.2 percent, respectively. With the relatively large number of points contained in these three figures, one can conclude that the thickness (total counts) is measurable to a statistical repeatability of approximately 25 percent and that the percent variation in mercury, cadmium, and tellurium is ±1 percent, ±0.5 percent, and ±0.6 percent, respectively. It should also be noted that the tellurium composition is relatively independent of the cold finger temperature whereas the cadmium, mercury, and thickness are indeed dependent on that temperature.

Similarly, a series of runs was made in which the growth time was the variable and in which one chip was held down firmly to the top of the growth pedestal by the second thermocouple housing. The results of this series of measurements are illustrated in Figure 5-4. Here, it is clear that within statistical limits the effect of more intimate contact of Chip #1 by the hold-down was insignificant. However, there is a significant variation in the results as the length of the growth time is increased. Specifically, the growth increases quite rapidly in thickness between one and two hours growth time. The hold-down (Chip #1) adds heat to the vicinity of the growth, modifying the composition slightly. Furthermore, the grain size increases as the time of the growth increases. Some of the apparent change in composition may be due to varying matrix self-absorption effects in the x-ray fluorescence measurements; however, this influence has not been measured. It is interesting that the growth continues to increase even at the longer times whereas the mercury content decreases significantly at these longer times. The percent sapphire cutoff is relatively independent of the growth time with good quality detectors being produced at all growth times (except at four hours) within the statistical repeatability of the data.

The cold finger temperature scan performed from Runs #CK-101 to CK-106 have not been completely evaluated at the time of this report; however, of the growths evaluated, 16 percent are Class A, 32 percent are Class B, and 52 percent are not classifiable.

Those Runs #CK-107 to #CK-109 which are initiated to test the effect of varying the growth furnace temperature while maintaining the cold finger temperature constant, were inconclusive and statistically insignificant because a system fracture interrupted the series of growths prematurely.

Preliminary efforts were also initiated during this reporting period to make growths upon alumina substrates (one-quarter inch by one-half inch by approximately 10 mils). It was the original intention of this series of growth runs to determine 1) whether the growth of mercury cadmium telluride could be made upon this substrate material;

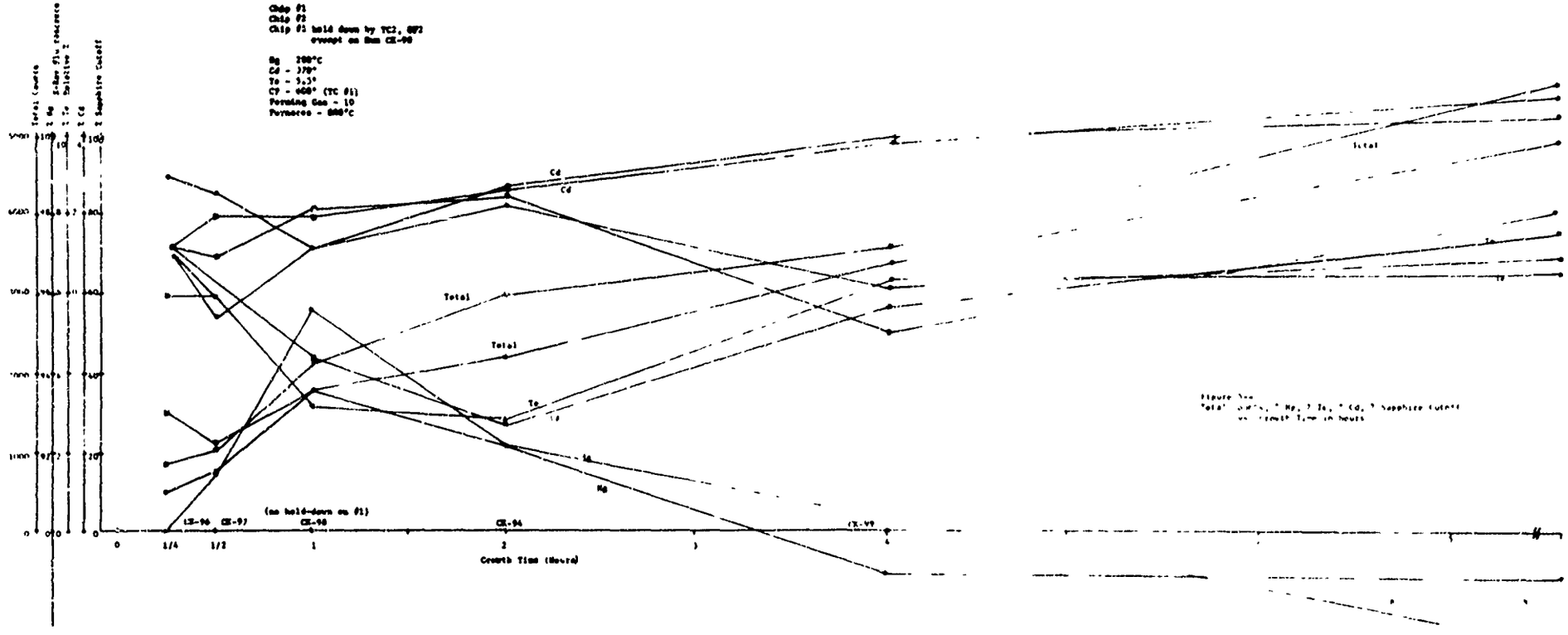

Figure [illegible]
"Total" Counts, % Mg, % Te, % Cd, % Sapphire Cutoff
vs. Growth Time in Hours

and 2) whether those resulting growths would show significantly improved adherence to the substrate over sapphire. These substrates had a fairly rough finish. Of the four growth attempts, involving seven alumina substrates, only one had significant sensitivity and percent sapphire cutoff, resulting in a Class C detector. The parameters of the growth system for that alumina were essentially the same as those used for the sapphire substrates but will, obviously, require some adjustments for optimization. This short series of growth runs demonstrated that detectors could indeed be made but more particularly demonstrated that the substrate's adhesion is very great. In fact, the porosity of the substrate made it quite difficult to scribe the detector lines of delineation so that they showed no conductivity. It is recommended that subsequent alumina substrates with a few micro-inch polish be used for this purpose. These will probably result in adequate adhesion without the difficulty of scribing.

The cadmium telluride growth on the surface of the alumina substrate is "visible" to the fluorescence x-ray through the 10-mil thickness of the alumina substrate when the growth is viewed from the backside of that substrate. A clean alumina substrate shows no evidence of mercury, cadmium, or tellurium peaks. It should also be noted that the alumina substrate turns a light brown under the integral x-ray radiation.

Of the eight runs made using cadmium telluride substrates, none showed significant detectivity, indicating that those growth parameters must be adjusted quite differently from the growth parameters used for sapphire. Because the substrate thicknesses were of the order of 7 to 10 mils and the substrates were extremely fragile, special mounting techniques were employed for the testing of these substrates. Briefly, they were placed within multi-lead flatpacks which were in turn soldered to the printed circuits for evaluation. Thus, if one of the substrates had shown significant sensitivity, justifying further testing, it could have been transferred directly to the dewar without further removal from the flatpack. Growths of the order of 0.3 mils were produced on top of these substrates, as evidenced by cross-sectioning and etching. At least two of the growths showed excellent epitaxial growth on the substrate; the single-crystalline nature of these epitaxial growths was confirmed by x-ray diffraction. No x-ray fluorescence analysis is possible on the cadmium telluride substrates because of the high background cadmium and tellurium peaks.

Two mercury cadmium telluride growths were made on barium fluoride substrates which had been polished for this purpose. These growths were polycrystalline.

Some interesting observations have been made microscopically (in reflection) upon the obvious growth orientation upon small areas of sapphire substrate. The sapphire substrates which have been used in these growths were not especially oriented; however, it is hypothesized by the supplier that some of the substrates may have the z-axis lying in the plane. The inter-atomic spacing along this axis is 12.6 A° being approximately twice the spacing of the subsequent cadmium telluride growth. This multiple spacing may give rise to the preferential growths which are observed microscopically. We have not been able to confirm the uniform orientation of these small areas by x-ray technology. With the indication that the sapphire substrate orientation affects the mercury cadmium telluride orientation, we can order oriented substrates for further study.

5.4 GROWTH OF MATERIAL (TEMPERATURE CONTROL OF COLD FINGER)

In these experiments, five series of epitaxial growths were undertaken, all on sapphire substrate, one-half inch diameter by 0.020" ± 0.001" in thickness. These five series of growths are contained in 38 runs upon 76 chips (half circles). Of these 38 runs, 27 chips from 16 runs were fully evaluated as detectors; in all, 128 detectors were fabricated and tested. The results of these tests are shown in Table 5-2.

Table 5-2

EVALUATION OF DETECTORS

Class	# of Chips	%
A	5	19
B	5	19
C	0	0
D	1	4
E	2	7
F	7	26
G	0	0
H	2	7
Not classified	5	19
Total	27	101

Evaluations on the remaining growths and detectors are underway but are incomplete at the time of this writing.

The general purpose of the five series of runs was 1) to test the hypothesis that good detectors could be grown by holding the cold

finger cooling air at a constant value (rather than holding the cold finger temperature at a constant value); 2) to test the effect on the resulting growth of scanning the cadmium source furnace temperatures at two different air flow rates; and 3) to vary the growth furnace temperature while maintaining the temperature gradient between the growth furnace and the cold finger constant, in order to determine the effect on the resulting detectors of varying growth temperature (at constant temperature gradient).

Runs #CK-127 to #CK-133 used constant air during each run while the cadmium furnace temperature was held at a coaxial temperature of 344°C (approximately 20° above melting). In this set of runs, the air was varied over a relatively wide range, giving a range of cold finger temperature from 524°C to 587°C. Similarly, Runs #CK-134 through #CK-142 were performed at a cadmium furnace temperature of 365°C, with the air being held constant throughout each individual run, at finer changes, and over a narrow range of air, producing 622° to 606° as the cold finger temperature. Runs #CK-142 through CK-152 were all made with the air flow constant at 40 air flow units (cold finger temperature 606 $\pm$ 10°C) and those Runs CK-153 to CK-158 were operated at a constant air flow of 46 air flow units (cold finger temperature (605 $\pm$ 3°C). In the first of these run series, at an air flow rate of 40, the coaxial cadmium source furnace temperature was varied in 10° steps from 310° to 400°C, while in the second series of runs at 46 air flow units, the cadmium temperature was varied from 330° to 380°C. In the fifth of these series of runs, for growth furnace temperature scans in Runs CK-159 through CK-165, the coaxial cadmium source temperature was constant at 370°C and the air was held constant at 40 units. In these series of runs, the growth furnace temperature was varied from the usual 800°C down to 700°C. Because of the constant cooling air, the gradient (differential between the growth furnace temperature and the cold finger pedestal top temperature) was remarkably constant at 196.5°C $\pm$ 0.5°C, except for the extreme temperatures of 800° and 700° where that gradient rose to 201.5°C and 206°C, respectively. Since the entire heating of the top of the growth pedestal is due to radiant heating and convective heating from the growth furnace, the constant cold finger air permitted a very uniform maintenance of the growth temperature gradients.

For all of these series of runs, the tellurium source furnace temperature was maintained at 522°C and the mercury furnace at 280°C.

5.4.1 COMPOSITION RESULTS (RELATED TO TEMPERATURE MEASUREMENTS)

This section reports only upon those growth parameters related to temperature measurements, air flow rate, and the composition of the resulting growth as measured by the fluorescence x-ray analysis. Under no circumstances are the relative percents quoted herein to be construed to represent true, quantitative percents of the constituents

reported. However, it is assumed that, in lieu of this absolute calibration, the relative changes indeed are representative of the bulk material.

Growths of epitaxial material upon sapphire, in which the cold finger temperature is held constant, require constant supervision and manual re-adjustment of the air flow rate to maintain that constant temperature. This is due to the fact that the entire heating of the substrate arises from the growth furnace and, as the growth progresses, especially in the first 90 seconds of the growth, the color (absorptivity and reflectivity) and the convective flow of gases result in a rapidly changing thermodynamic equilibrium situation. In an effort to make the growth operation more automatic (and, hopefully, more reliable), efforts were made to determine whether the same high-class detectors should be made at constant air. As a result of the measurements, it is clear that of the detectors evaluated at least as large a percent of the detectors fabricated are of Class A and B quality with constant air as with the more difficult to maintain constant cold finger temperature. Only a statistical study can compare and establish with certainty whether the constant air or constant cold finger temperature produces a larger percentage of higher quality detectors.

There has been some concern about the nature of the approach to temperature equilibrium of the cold finger temperature when the air flow rate to the cold finger is maintained constant. After the air is first turned on, this temperature drops radically, reaching a minimum in about 90 seconds, and then rises 15 to 20° over the course of the two-hour growth, with most of the temperature rise occurring in the first fifteen minutes. (It was reported in the previous quarterly progress report that some significant growths are produced after only 15 minutes.) The relationship between the temperature equilibrium after two hours growth and after only one hour growth as a function of air flow rate is illustrated in Figure 5-5. In this curve the ultimate asymptotic peak cold finger temperature is within $2° \pm 1°C$ of the temperature of the cold finger after only one hour growth.

For Runs #CK-127 through CK-133 the variation in the percent mercury, cadmium, and tellurium and the total number of counts (as determined by x-ray fluorescence) are plotted as a function of air rate in Figures 5-6, 5-7, and 5-8. Similar computer-generated curves for Runs #CK-134 through CK-142 show essentially the same variations except that those runs were executed over a narrower range of air flow rate and at a higher cadmium source furnace temperature. Moreover, curves showing these parametric variations with cold finger temperature (Figures 5-9 and 5-10) display essentially the same (inverse) relationships. The variation from run to run and from Chips 1 and 2 (opposing halves of the same run) are clearly illustrated in the extremes of the variation of these curves; for example, the variation in mercury percent is of the order of ± 0.8 percent; for tellurium,

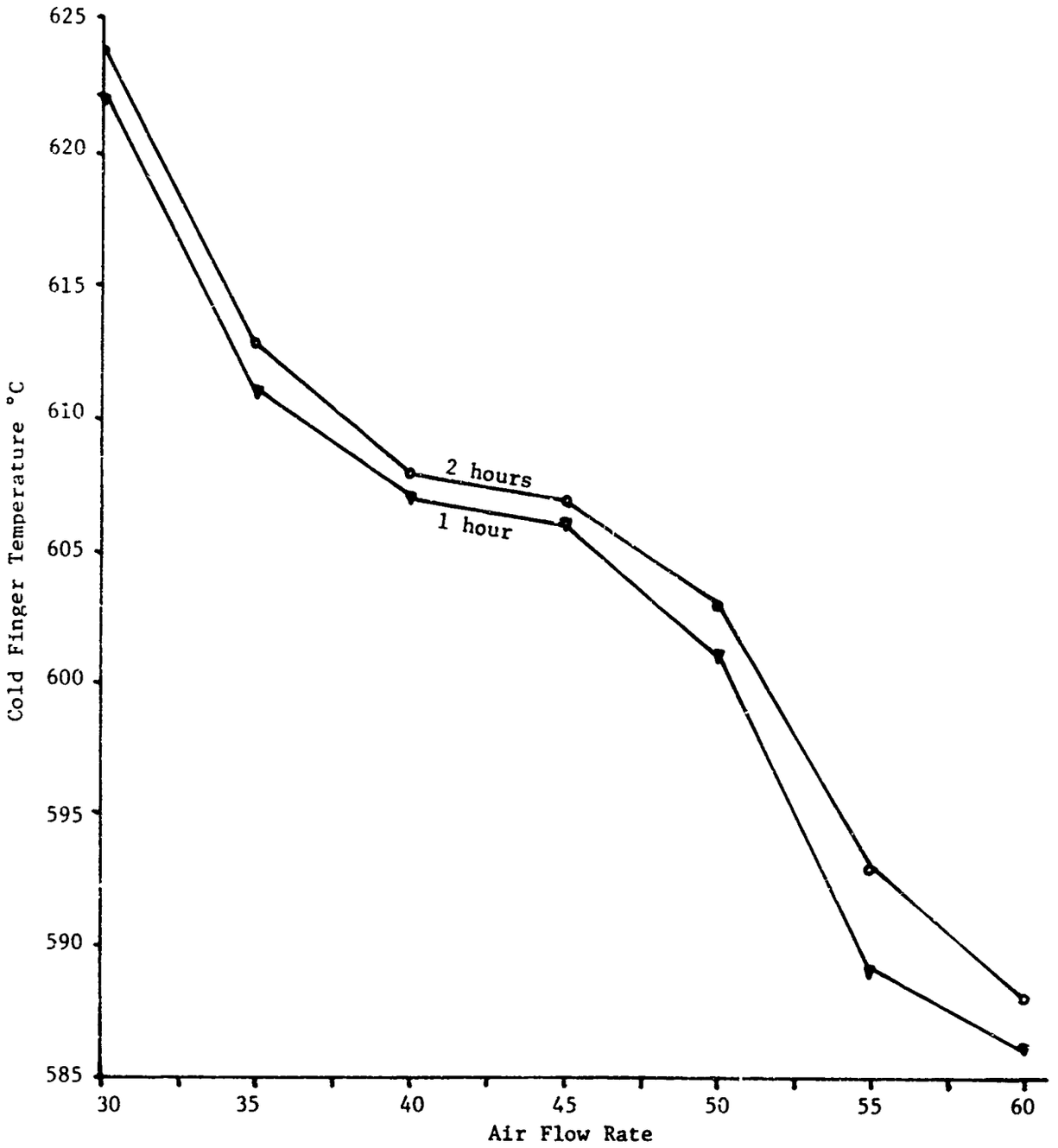

Figure 5-5
Cold Finger Temperature vs. Air Flow Rate

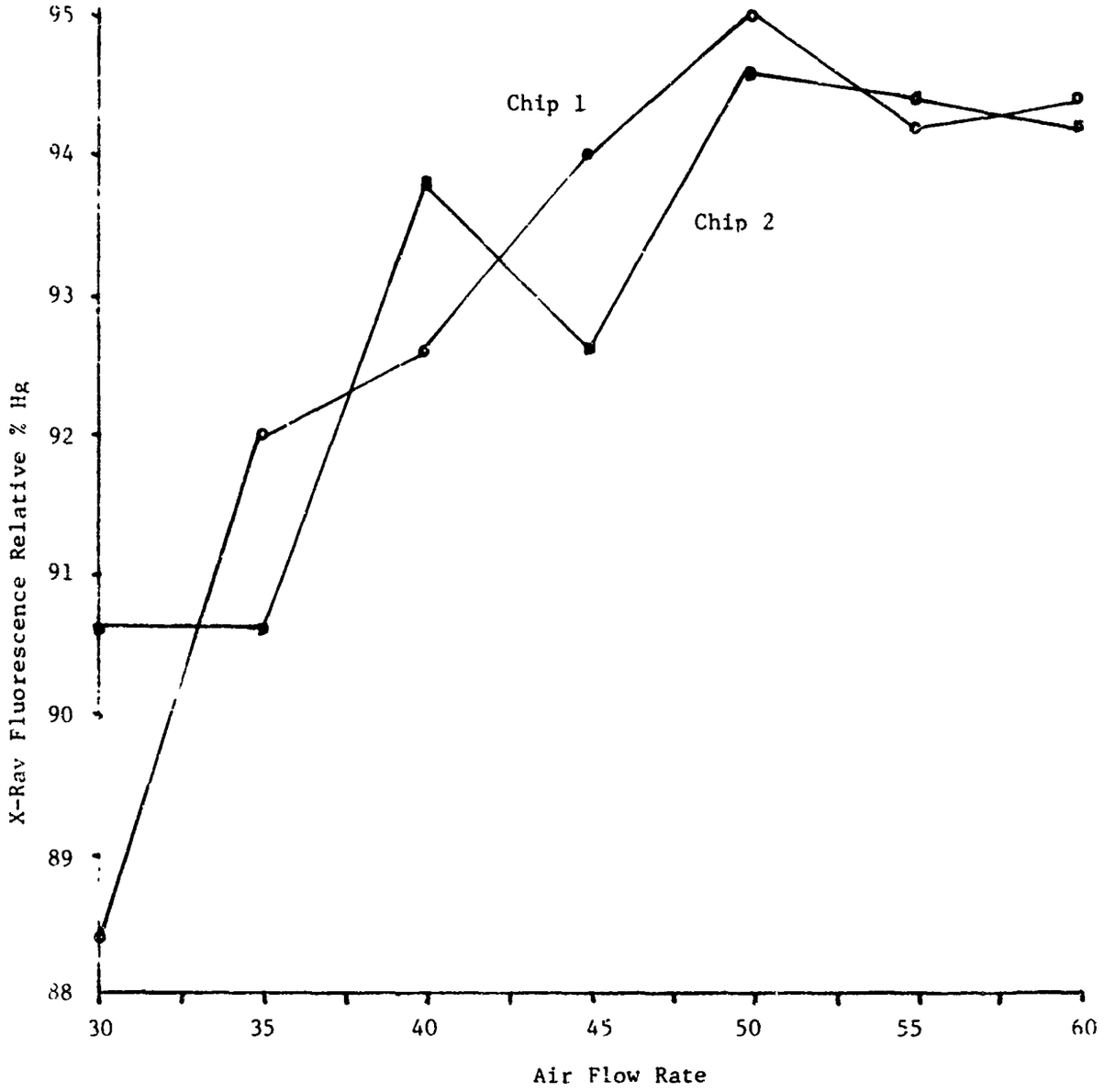

Figure 5-6
Relative Percent Hg vs. Air Flow Rate

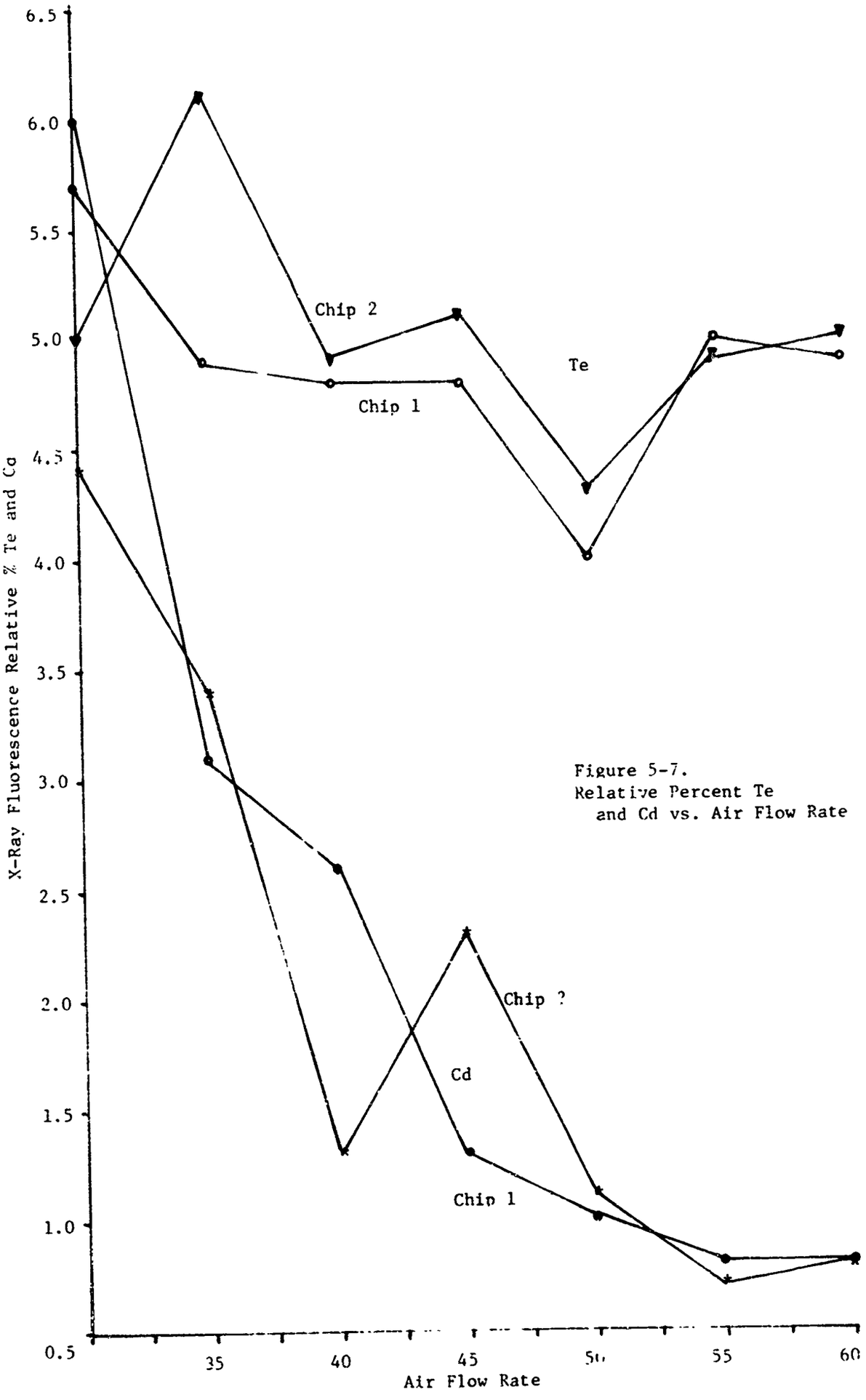

Figure 5-7.
Relative Percent Te
and Cd vs. Air Flow Rate

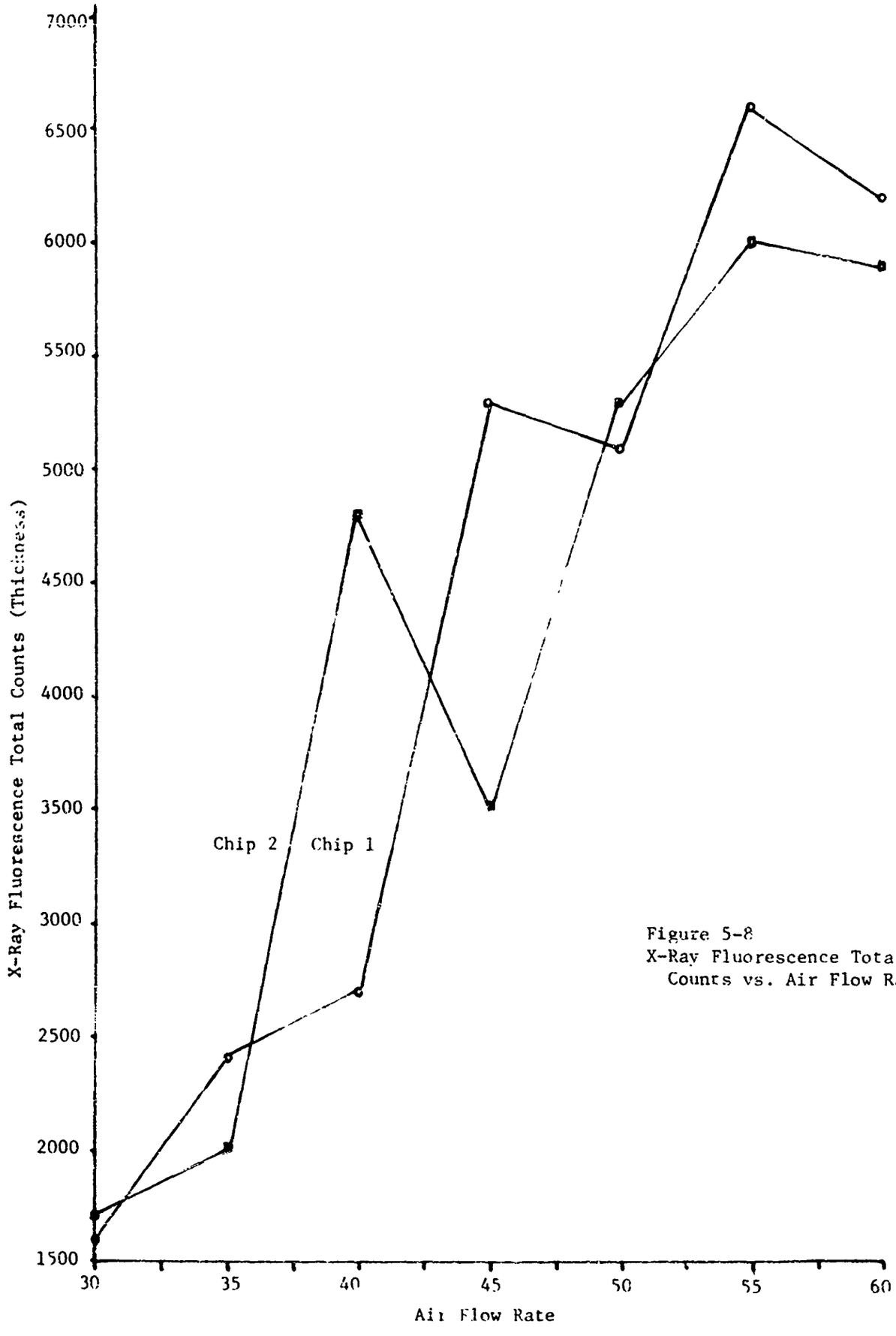

Figure 5-8
X-Ray Fluorescence Total Counts vs. Air Flow Rate

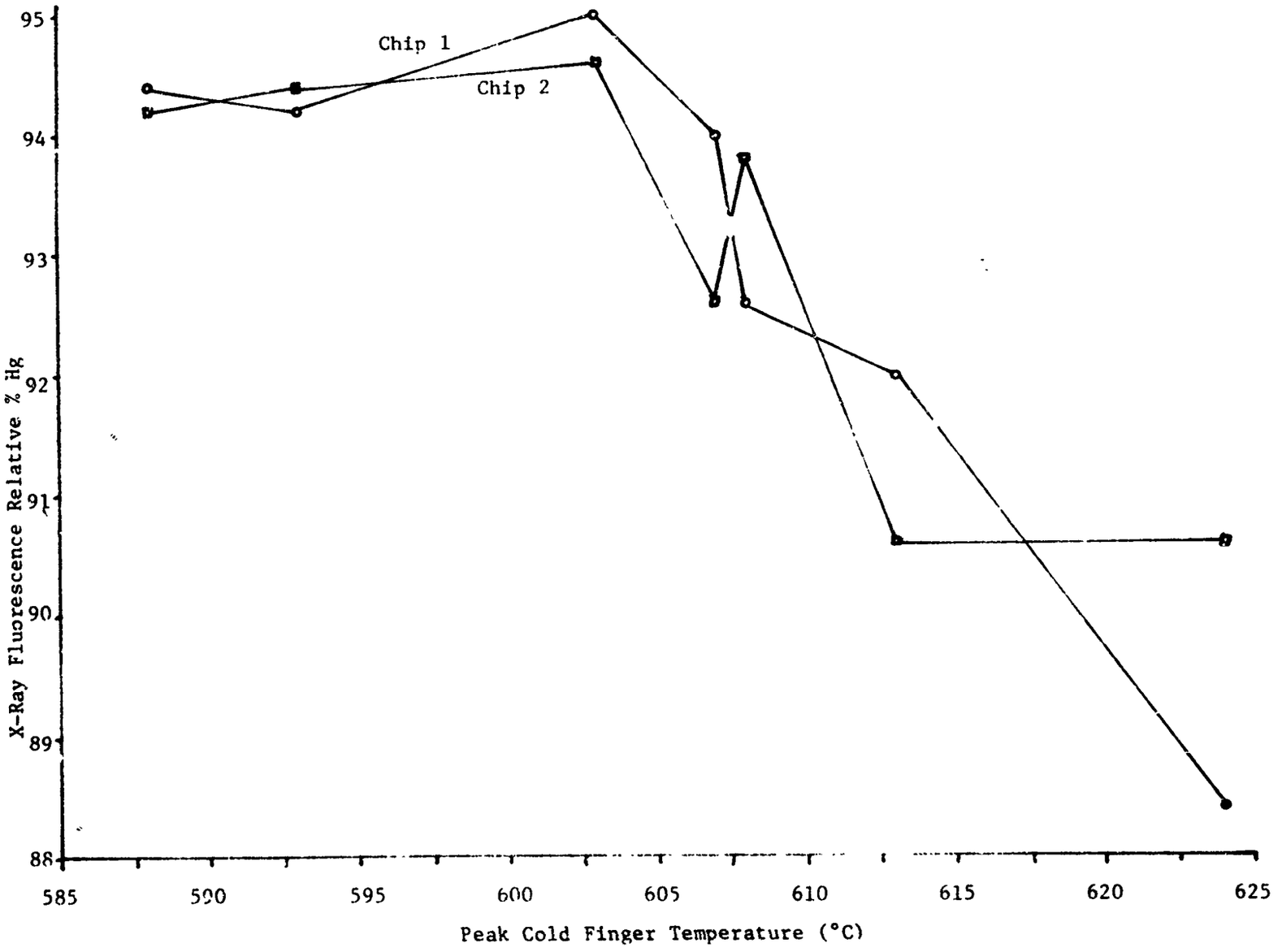

Figure 5-9
Relative Percent Hg vs. Peak Cold Finger Temperature

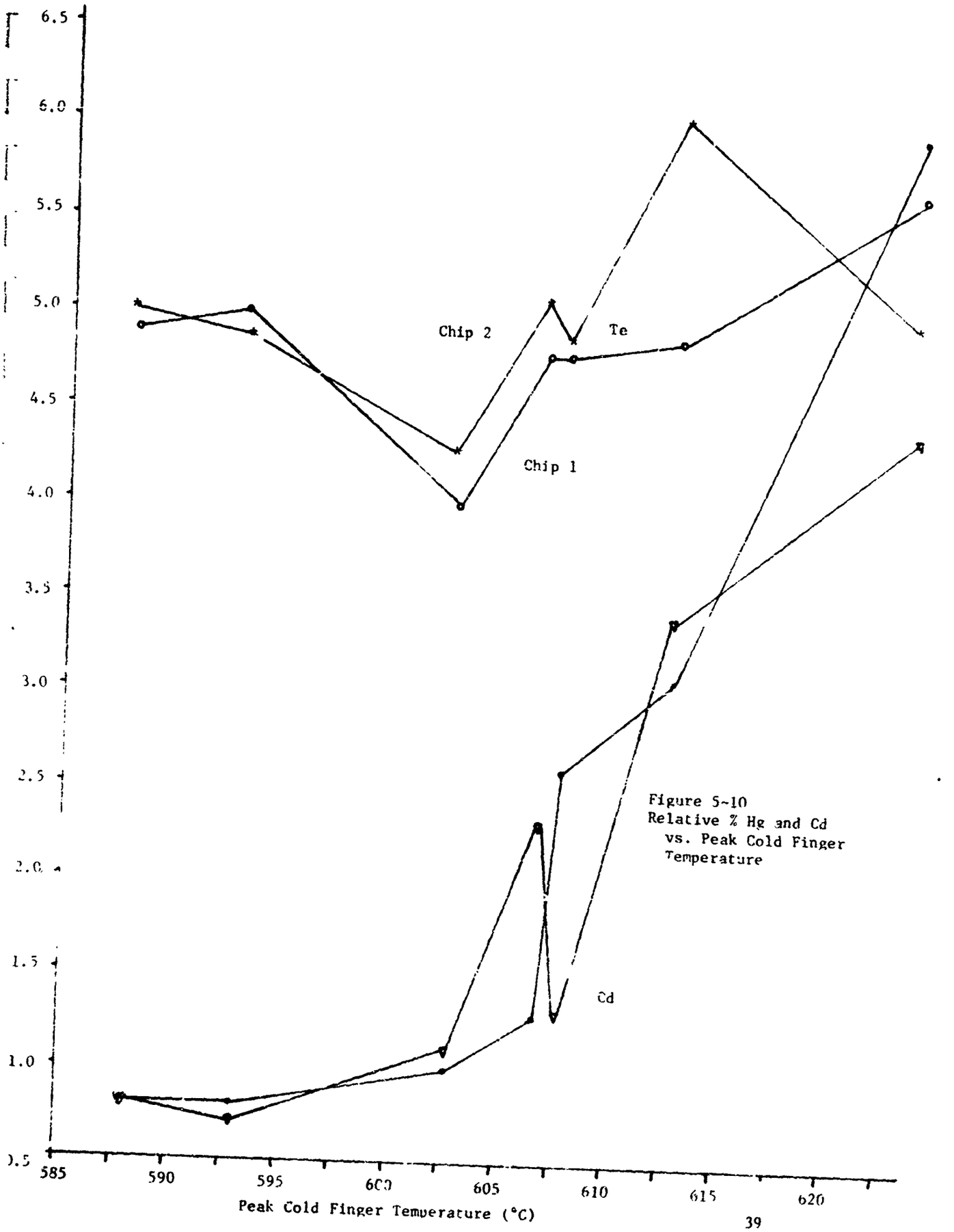

Figure 5-10
Relative % Hg and Cd
vs. Peak Cold Finger
Temperature

±0.5 percent or less; and for cadmium, ±0.5 percent. We assume a direct relationship between the total counts (Figure 5-8) and the thickness of the resulting growth; variations in thickness from run to run are approximately ±1,000 counts or approximately 25 percent. No crystal perfection data are illustrated in these curves.

Other correlations between the parameters were studied. It is shown in Figure 5-11, wherein the mercury content is compared with the cadmium content in all of the chips in all of the runs from CK-127 through CK-142, that there is a definite reduction in the mercury as the cadmium rises, as should be expected. Other plots of the data show that the tellurium is relatively constant and is not a significant function of either the cadmium or mercury content, as again should be expected.

A careful statistical study of the composition of Chip 1, which was always maintained at the same position on the cold finger, as compared to Chip 2 (oppositely oriented) shows that the mercury data are reliable to ±0.8 percent and that the Chips 1 have more mercury, as indicated by a colder cold finger in that position. The cadmium data are ±1.0 percent, and there is no statistical difference between the cadmium content of Chips 1 and 2; and the tellurium data are shown to lie within ±1.0 percent composition but there is a definite indication that Chips 2 have more tellurium. It is interesting to note that all the tellurium composition is clustered in the range of 4.75 to 7.0 percent, regardless of the conditions of growth, over a wide range of parametric changes. The total counts data vary by ±600 counts or about 20 percent in these data and show that Chips 1 are somewhat thicker. In order to alleviate this real difference between chips located at Position 1 on the cold finger and Position 2 on the cold finger, whole sapphire discs were used. All runs following CK-142 have been performed on pre-scribed, whole discs of sapphire, permitting the growths to be made upon an entire disc, the growths to be measured for composition by x-ray fluorescence, and then the chips to be broken along a diameter. It is hoped that this procedure will give more uniform growths across the diameter of the chips. This variation at the edge (edge-effect) is also evidenced by the observation that the sapphire cutoff and signal-to-noise ratio have heretofore shown greater variations than those three detectors in the central portion of the half-circle.

5.4.2 RESULTS OF COMPOSITION ON PRE-SCRIBED CHIPS

Figures 5-12, 5-13, and 5-14 show the improved compositional results of this technique. In these figures, the 1 and 2 designate chip numbers whereas M designates x-ray fluorescence measurements made in the middle of the pre-scribed discs. By using this technique, the mercury measurements are valid ±0.7 percent: the cadmium, ±0.5 percent; and the tellurium, ±0.6 percent. In addition, the total

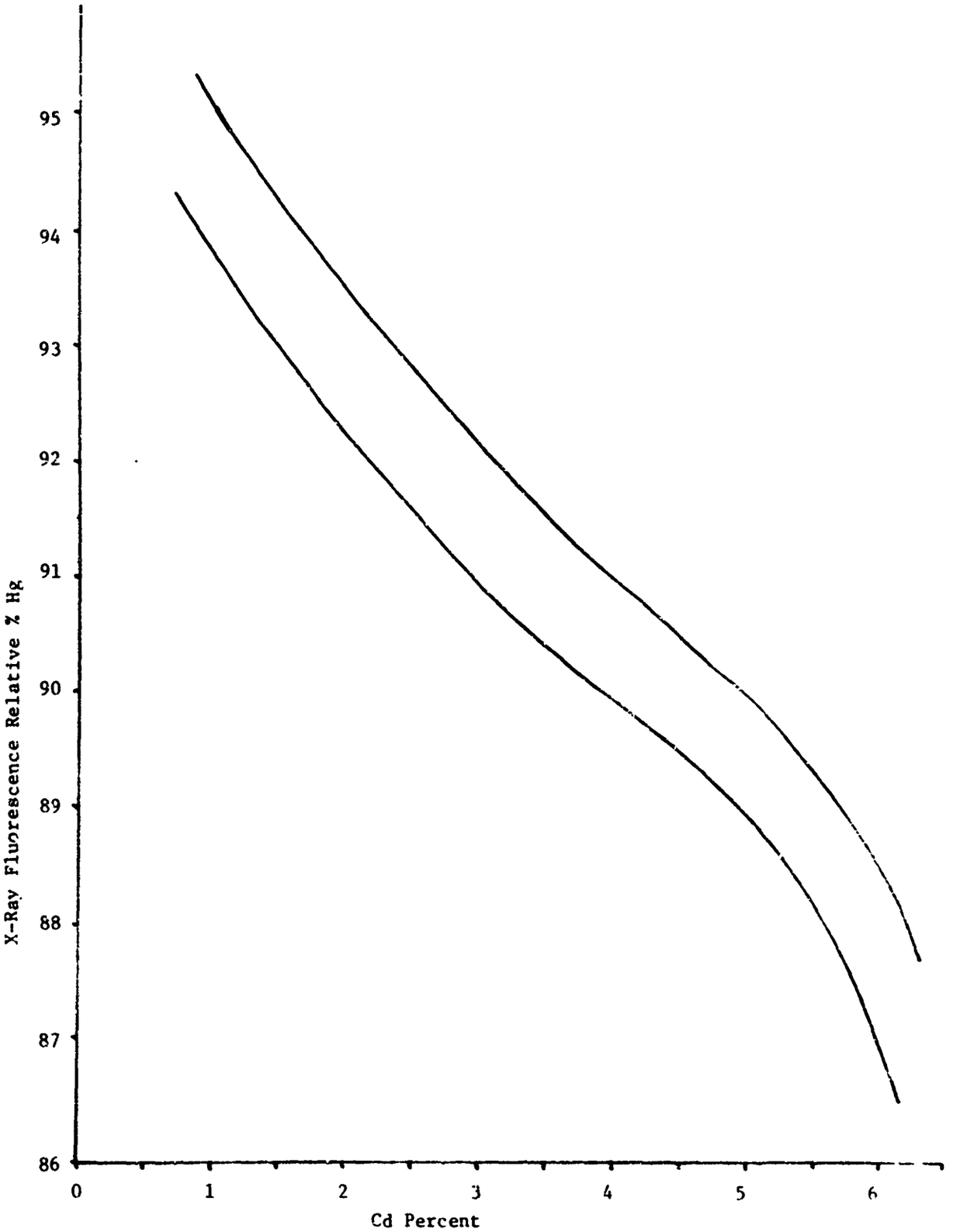

Figure 5-11
Relative % Hg vs. % Cd (All Chips and Runs Combined)

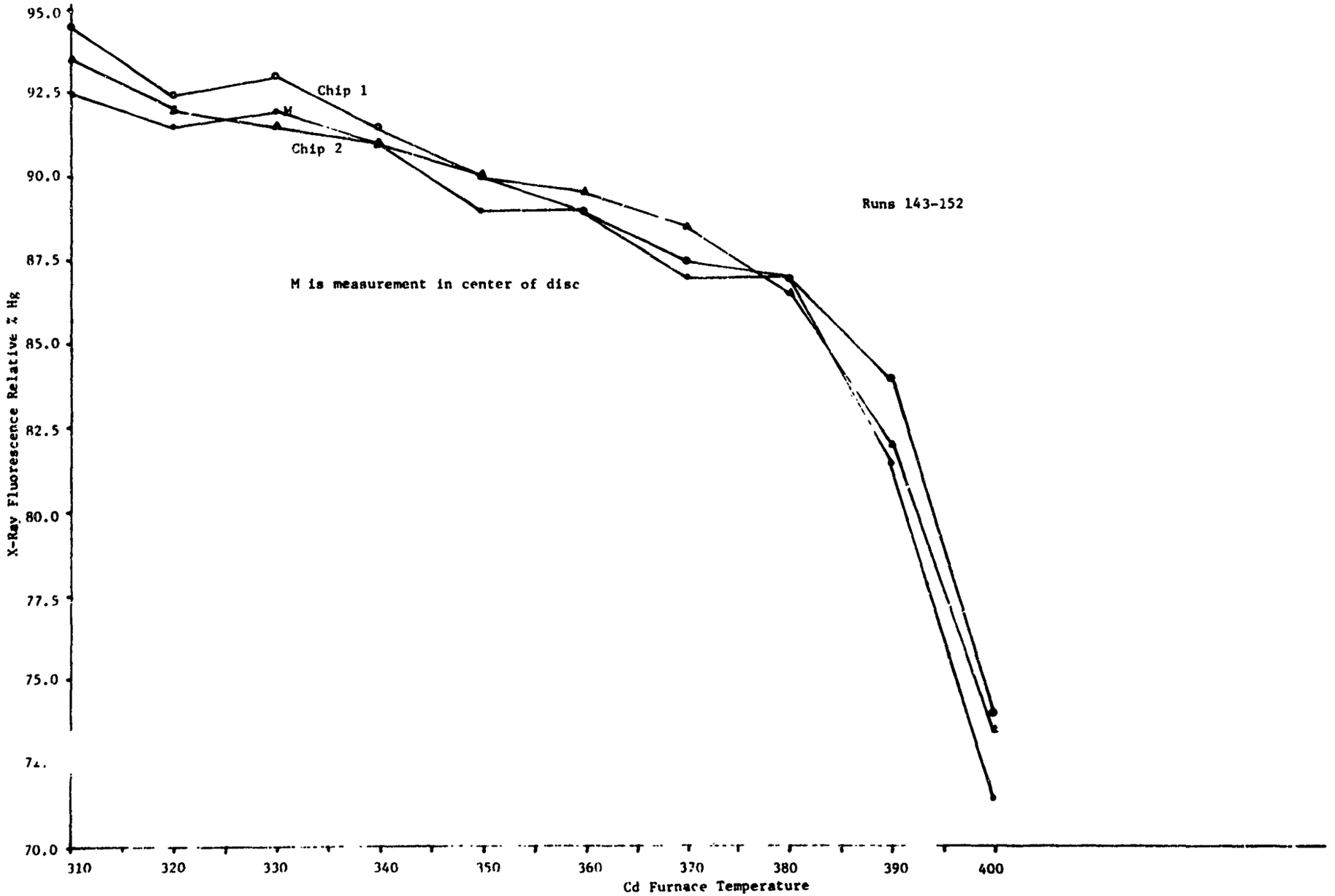

Figure 5-12
Relative Percent Hg. vs, Cd Furnace Temperature

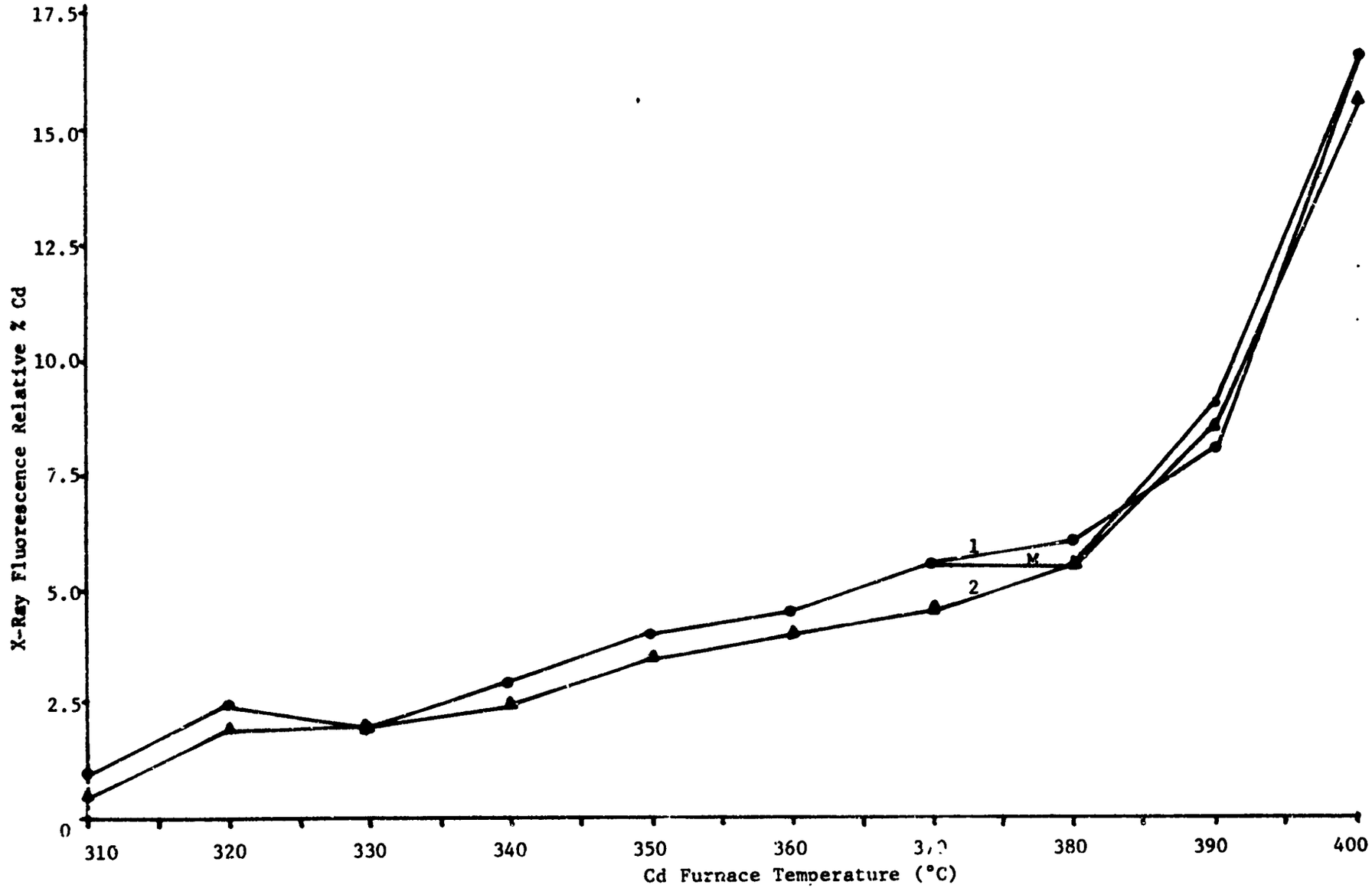

Figure 5-13
Relative Percent Cd vs. Cd Furnace Temperature

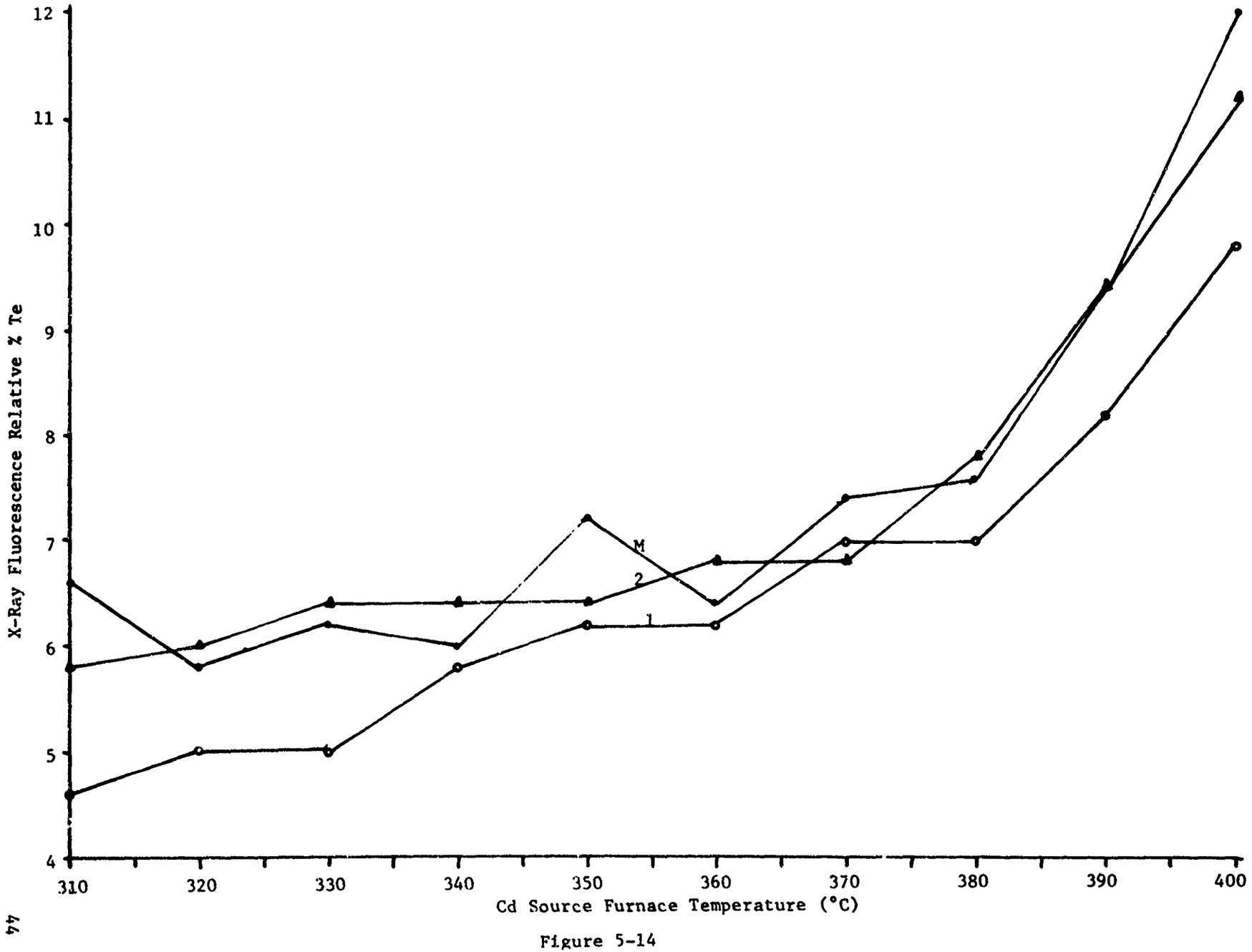

Figure 5-14
Relative Percent Te vs. Cd Source Temperature

counts uncertainty has been reduced to about ±15 percent. Again, a definite relationship exists between the cadmium and the mercury and between the tellurium and the mercury as illustrated in Figure 5-15, wherein the cadmium and tellurium percents are plotted as functions of the mercury percent.

A rather surprising result of the two series of runs, CK-143 through CK-158, in which the coaxial cadmium source furnace temperature was varied, while the air was set at two different values, was that in the case of the lower air (hotter cold finger temperature) the thickness (total counts) of the growths reached a maximum in the region of the cadmium furnace temperature of 380° to 390°C whereas, at 46 air flow units (colder cold finger) there was a rather monotonic decrease in thickness as the cadmium source furnace temperature was raised. Figures 5-16 and 5-17 compare the compositional results for mercury, cadmium, and tellurium at the two different cold finger temperatures as functions of the cadmium source furnace temperature. In these, the tellurium is relatively independent of the air; the cadmium content increases with increasing cold finger temperature. Thus, it is apparent that one can vary the cadmium and mercury percentages by either a variation of the cold finger temperature or by variation of the cadmium source furnace temperature; and furthermore, the tellurium is dependent upon the cadmium source furnace temperature but is relatively independent of the cold finger temperature.

The compositional results of the variation of the growth furnace in Runs CK-159 through CK-165 are illustrated graphically in Figures 5-18, 5-19, and 5-20. The mercury composition dropped as the growth furnace temperature rose (the temperature gradient between the growth furnace and the cold finger was maintained constant at approximately 200°C), whereas the cadmium rose with increasing growth furnace temperature; as before, the tellurium was independent of this parameter. Cadmium changed from 5.5 percent at mercury of 87.5 percent to a cadmium percent of 2.4 percent at mercury of 90.7 percent.

One interesting conclusion of these curves is that the maximum thickness of growth occurs at approximately 750° growth furnace temperature with these source furnace parameters. It will be desirable to determine that this thicker growth will in fact result in more satisfactory detector material.

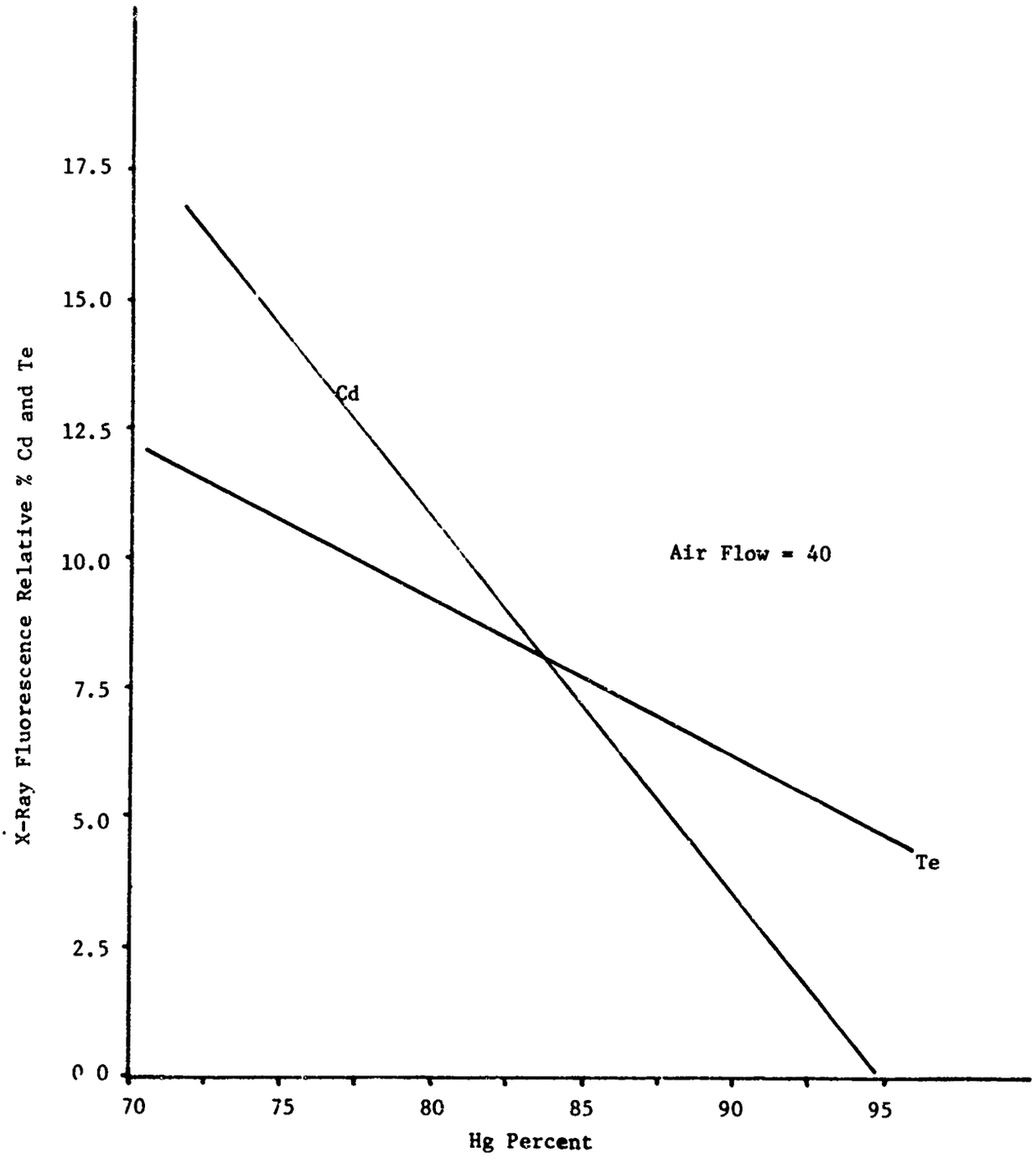

Figure 5-15
Relative Percent Cd and Te vs. Hg Percent
(Runs 143 through 152)

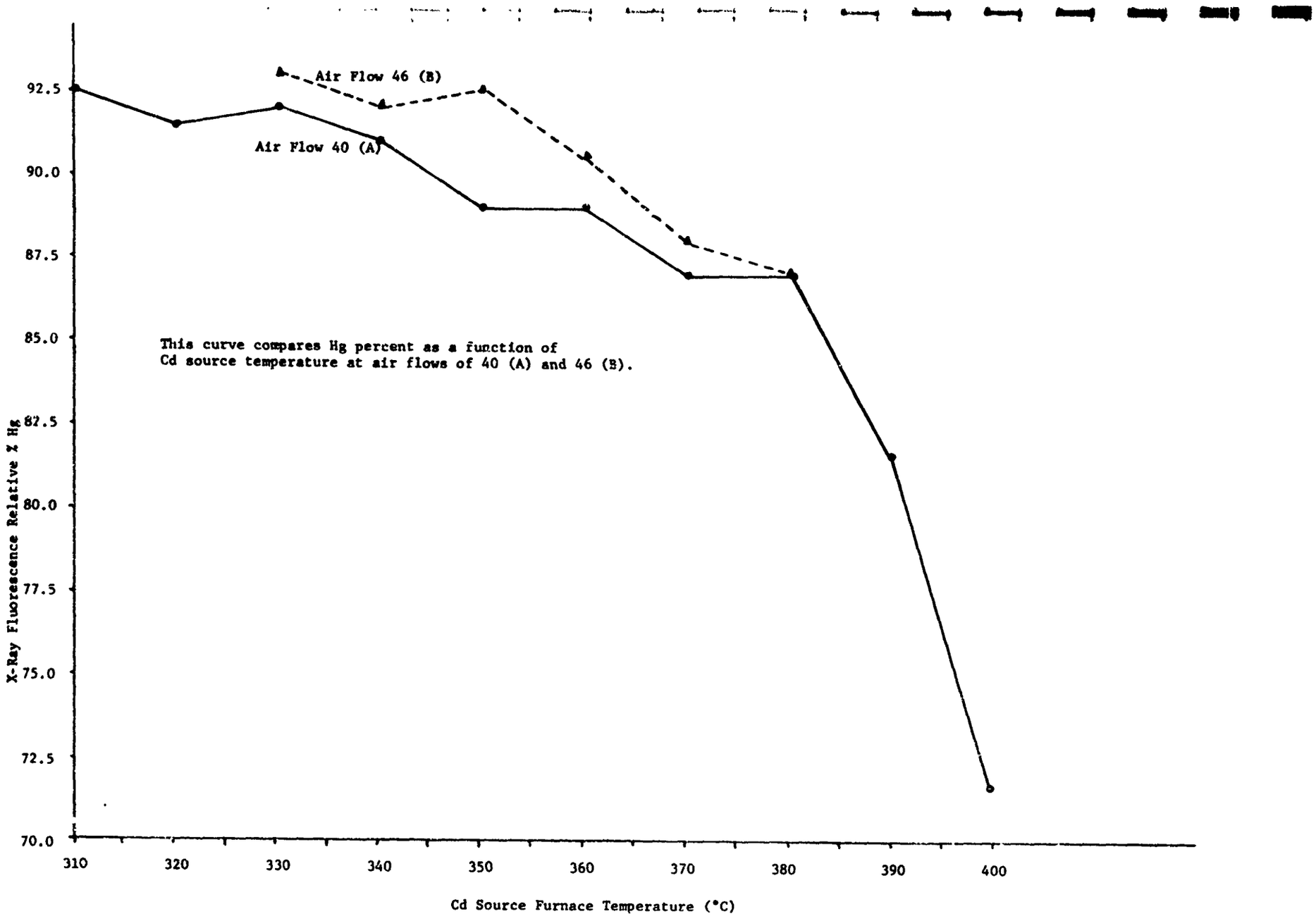

Figure 5-16
Relative Percent Hg vs. Cd Source Furnace Temperature

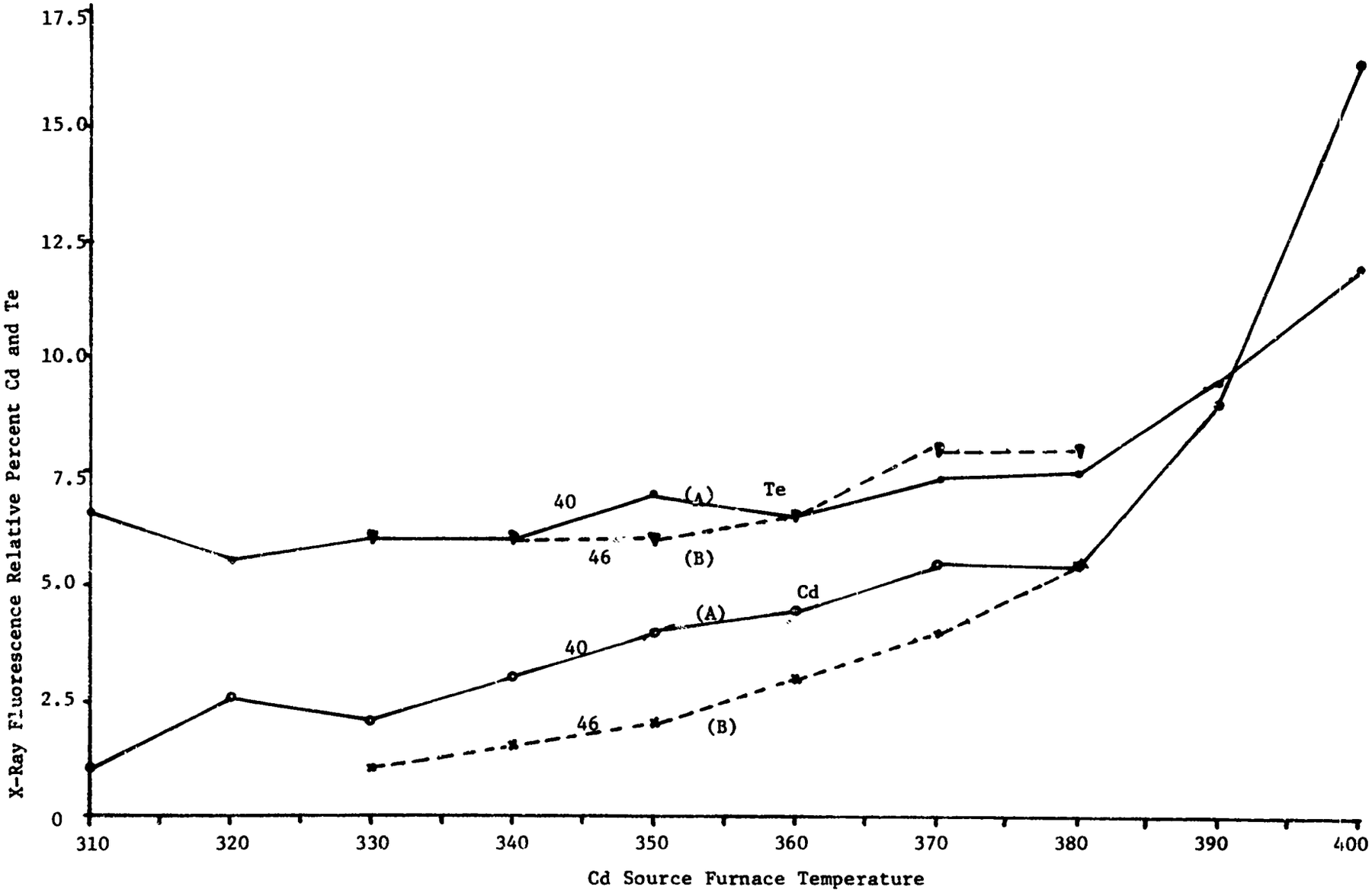

Figure 5-17
Relative Percent Cd and Te vs. Cd Source Furnace Temperature

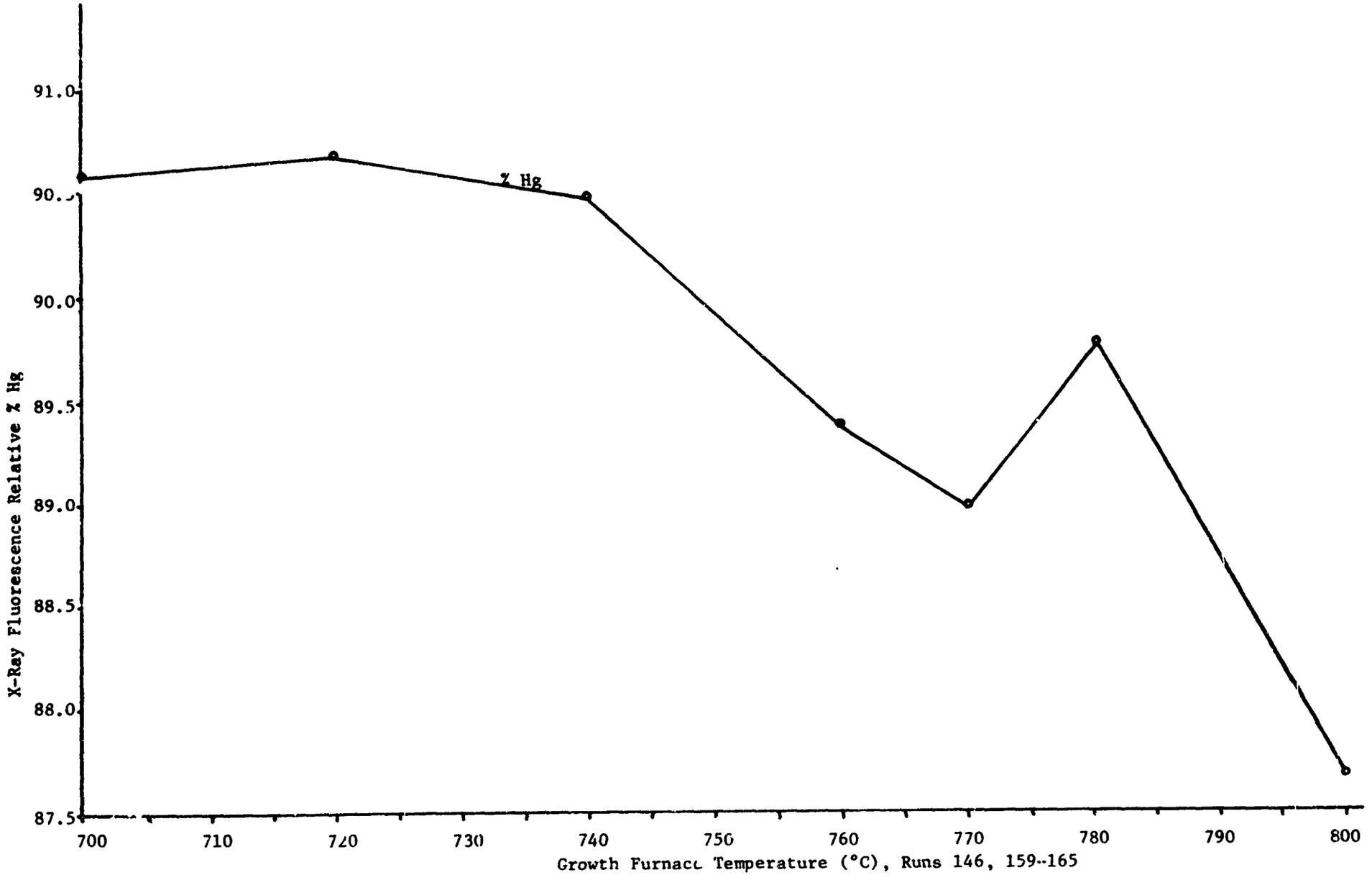

Figure 5-18
Relative Percent Hg vs. Growth Furnace Temperature

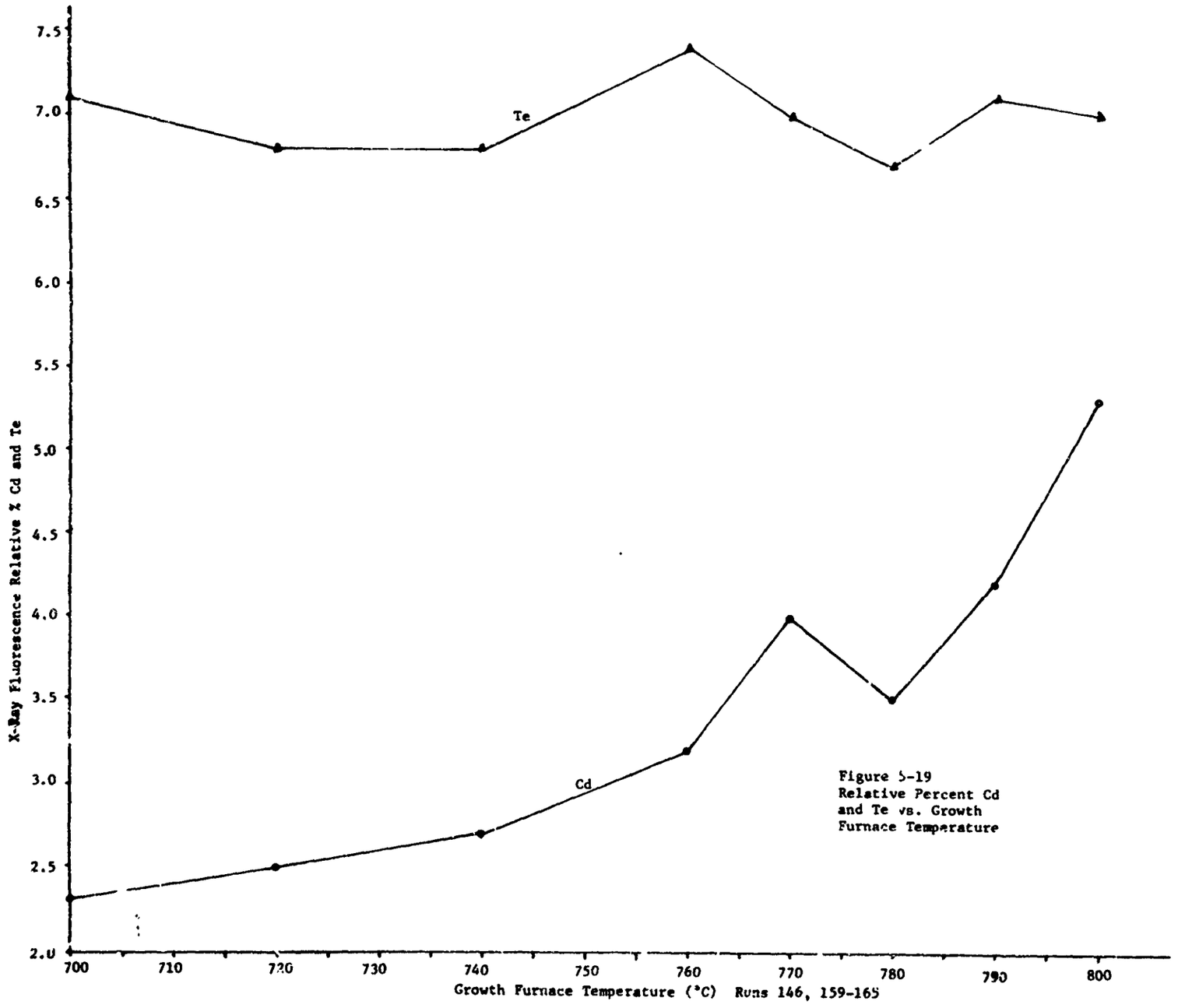

Figure 5-19
Relative Percent Cd
and Te vs. Growth
Furnace Temperature

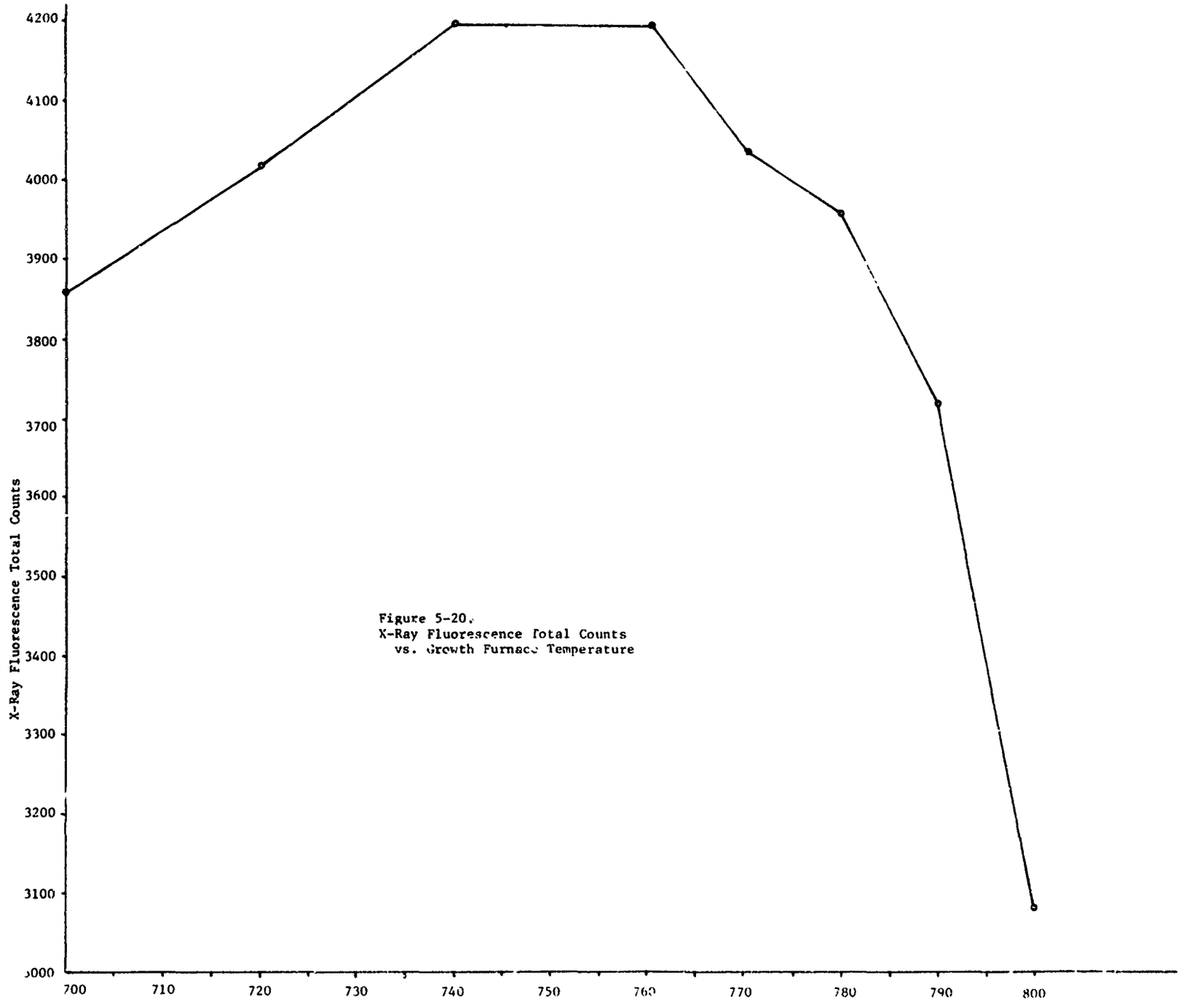

Figure 5-20.
X-Ray Fluorescence Total Counts
vs. Growth Furnace Temperature

Section 6

DETECTOR EVALUATION

6.1 LEAD ATTACHMENT

During the past year, many experiments were performed in order to produce a good method for attaching leads to the HgCdTe material. As a result of these experiments, it was concluded that, to date, the most reliable and successful lead attachment methods require the covering of the HgCdTe material with evaporated gold before either thermocompression bonding or silver epoxy on sapphire substrates can be attempted. It was further concluded that gold evaporated leads and lead-outs can be used to provide conduction paths over the edge of scribed material to conductive pads for various methods of ancillary lead attachment.

6.2 MEASUREMENT OF RESISTIVITY BY FOUR POINT PROBE

It is expensive and time-consuming to evaluate the electrical characteristics of the grown mercury cadmium telluride by gold evaporation and lead attachment. In an effort to simplify the contacting for electrical characterization without the laborious lead attachment, we have attempted to use a four-point probe. This probe operates with good repeatability and reliability on gold evaporated surfaces plated on glass or sapphire and on gold evaporated over the growths on sapphire, giving only small surface damage. However, with the probe at hand, the contact to the cadmium telluride indicated a sensitivity to varying pressure and, because the cadmium telluride substrates were so fragile, frequently broke those substrates unless special care was taken that they lie flat. The probe is presently being modified in further efforts to simplify this electrical evaluation. However, it is not anticipated that the probe will be particularly useful at liquid nitrogen temperatures.

6.3 DETECTOR MEASUREMENTS

The standard measurements made on HgCdTe detectors are detectivity (D*) and spectral response, both at 77°K. Special measurements have included response time and noise spectrum from 100 Hz to 50 KHz. Improvements in D* from 10^7 to low 10^9 have been realized this year. The peak of spectral response has been extended to 12 microns. Also, an improvement in the uniformity of material has been shown by the close agreement of the peaks of spectral response on several adjacent detectors on the same substrate. Response times of polycrystalline HgCdTe has been measured and found to be less than 20 nanoseconds and in some cases as low as 4 nanoseconds. A reduction in bias current

noise and a lower frequency limit of this type of noise (1/f) has been achieved in some cases.

The following data are representative of the state-of-the-art in polycrystalline HgCdTe and present details of measurement in the abovementioned areas.

A summary of measurements made on 24 polycrystalline detectors grown on nine sapphire substrates is shown in Table 6-1. The spectral response of detectors on three substrates is shown in Figure 6-1, 6-2, and 6-3. It should be noted that Detector 94-1-C has a D* (500, 1000) in the low 10^9 region with a peak of response at 9 microns. The D* can be improved if a higher chopping frequency is used. For instance, 94-1-C has a D* of 10^{10} at 50 KHz.

Detectors 94-1-A, B, and C were tested at Syracuse University for D*, response time, and noise spectrum. They found the D*'s to be a factor of approximately 2 less than IBM's measurements. The response time was measured at 10.6 microns with a pulsed CO_2 laser. The rise time was found to be in the 20- to 50-nanosecond range and the decay time was 25 to 100 nanoseconds. This is shown for one detector, 94-1-C, in Figure 6-4. The noise spectrum for Detectors 94-1-A, B, and C is shown in Figure 6-5 along with the noise spectrum of the Texas Instrument FET preamplifier used in the measurements.

The noise spectrum of 94-1-C was replotted subtracting out the noise of the preamplifier. This is shown in Figure 6-6.

Figure 6-7 shows the noise spectrum of Detector 94-2-B measured at IBM and compared with the noise spectrum of a "good" single crystal Mullard HgCdTe detector. It should be noted that the Mullard detector has 1/f noise to 500 Hz, while the IBM detector has 1/f noise to 5 KHz. Beyond 5 KHz, the IBM detector's G-R noise is only slightly greater than the Mullard detector.

Table 6-1

CHARACTERISTICS OF HgCdTe DETECTORS ON SAPPHIRE SUBSTRATES
(Each Detector 0.5 x 1 mm)

Growth Number CK-1		ohms R 300°K	R 77°K	% Cutoff Vycor	Sapphire	Responsivity V/W	ma	D* (500, 1000) cm $Hz^{1/2}$ x w^{-1}	λ Peak Microns	Comments
76-1	A	12	28	95	82	3	25	1.2×10^8	~9	Very low noise, even at 25 ma. Sent to R. Jensen, NOL, 9-2-69.
	B	5	5	--	--			5×10^6		
	C	4	3	--	--			No signal		
76-2	A	47	150	96	82	20	20	1.5×10^8	9	
	D	20	59	95	83	6	20	1.1×10^8	12	
78-2	A	80	530	94	78	38	6	9.7×10^7	8	Sent to H. Weider, Corona Lab, 9-26-69, for x-ray analysis.
	B	38	186	95	82	68	25	9.1×10^7	11	
	C	46	340	95	82	123	25	1.3×10^8	9	
83-1	A	24	166	94	74	2.0	10	7.1×10^7	~8	
	B	15	100	88	66	2.6	15	1.3×10^8	~7	
	C	11	64	94	76	1.5	15	1.3×10^8	~8	
89-2	A	26	100	97	86	16	20	2.2×10^8	~12	For R. Jensen, 12-69.
	B	34	91	96	86	7	20	1.5×10^8	~12	
	C	55	174	96	86	17	20	1.9×10^8	~12	
91-1	E	30	80	96	84	8	20	7.5×10^7	~12	
94-1	A	62	57	92	66	125	20	8.1×10^8	7	
	B	44	44	93	75	66	20	1.0×10^9	7	
	C	31	34	94	76	71	20	1.6×10^9	9	
94-2	A	60	138	93	71	62	20	1.5×10^8	8	
	B	32	81	95	81	34	20	2.9×10^8	11	
	C	42	80	94	76	34	20	2.2×10^8	9	
100-2	A	48	530	96	82	150	12	7.0×10^8	~11	
	B	30	530	96	84	65	12	3.0×10^8	~12	
	C	72	2.6K	95	77	70	12	1.7×10^8	~ 9	

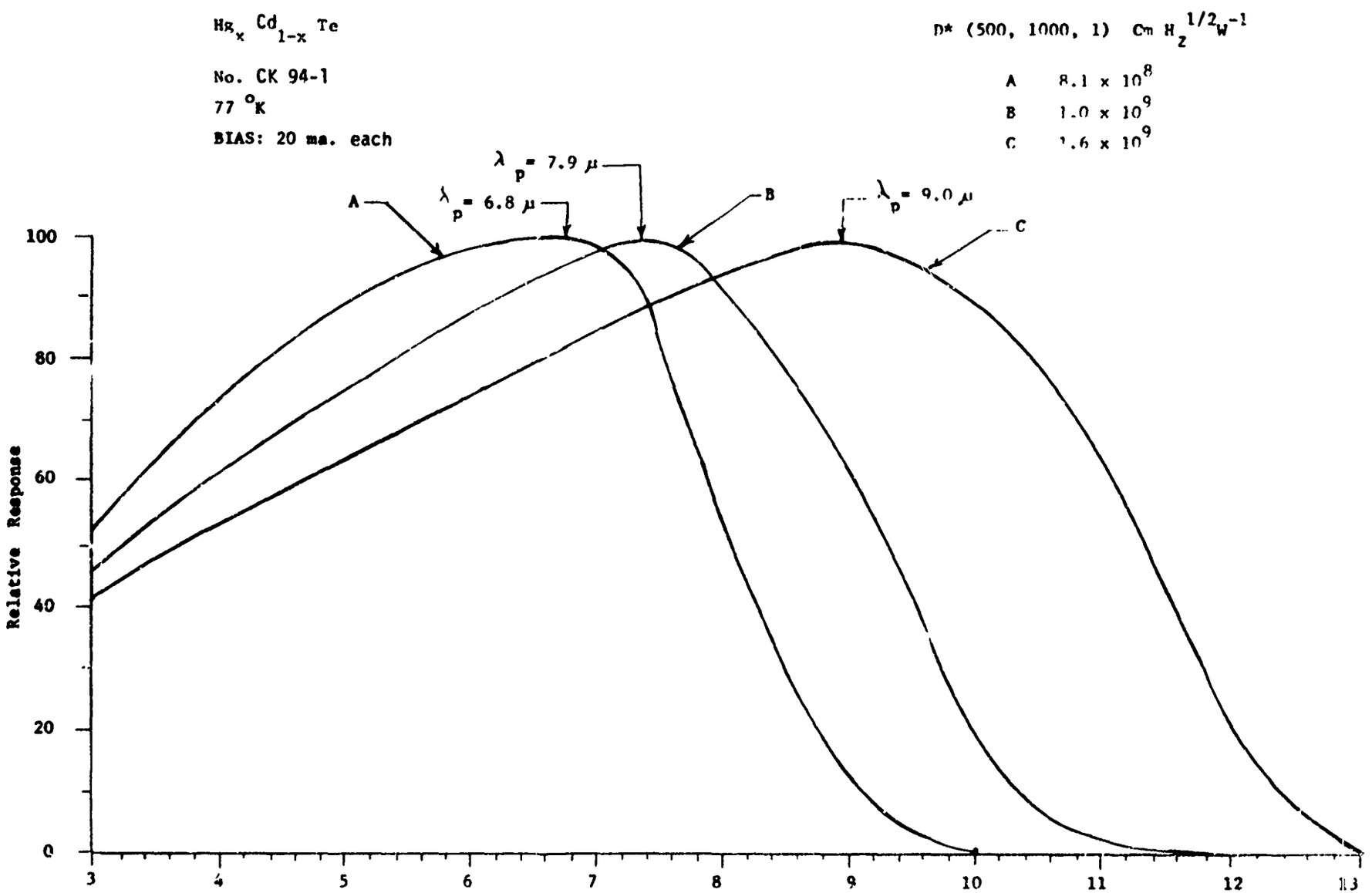
$Hg_x Cd_{1-x} Te$
No. CK 94-1
77 °K
BIAS: 20 ma. each
D* (500, 1000, 1) Cm $H_z^{1/2} W^{-1}$
A 8.1 x 10^8
B 1.0 x 10^9
C 1.6 x 10^9
λ_p = 7.9 μ
λ_p = 6.8 μ
λ_p = 9.0 μ
A
B
C
Relative Response
100
80
60
40
20
0
3
4
5
6
7
8
9
10
11
12
13
Wavelength - Microns

Figure 6-1

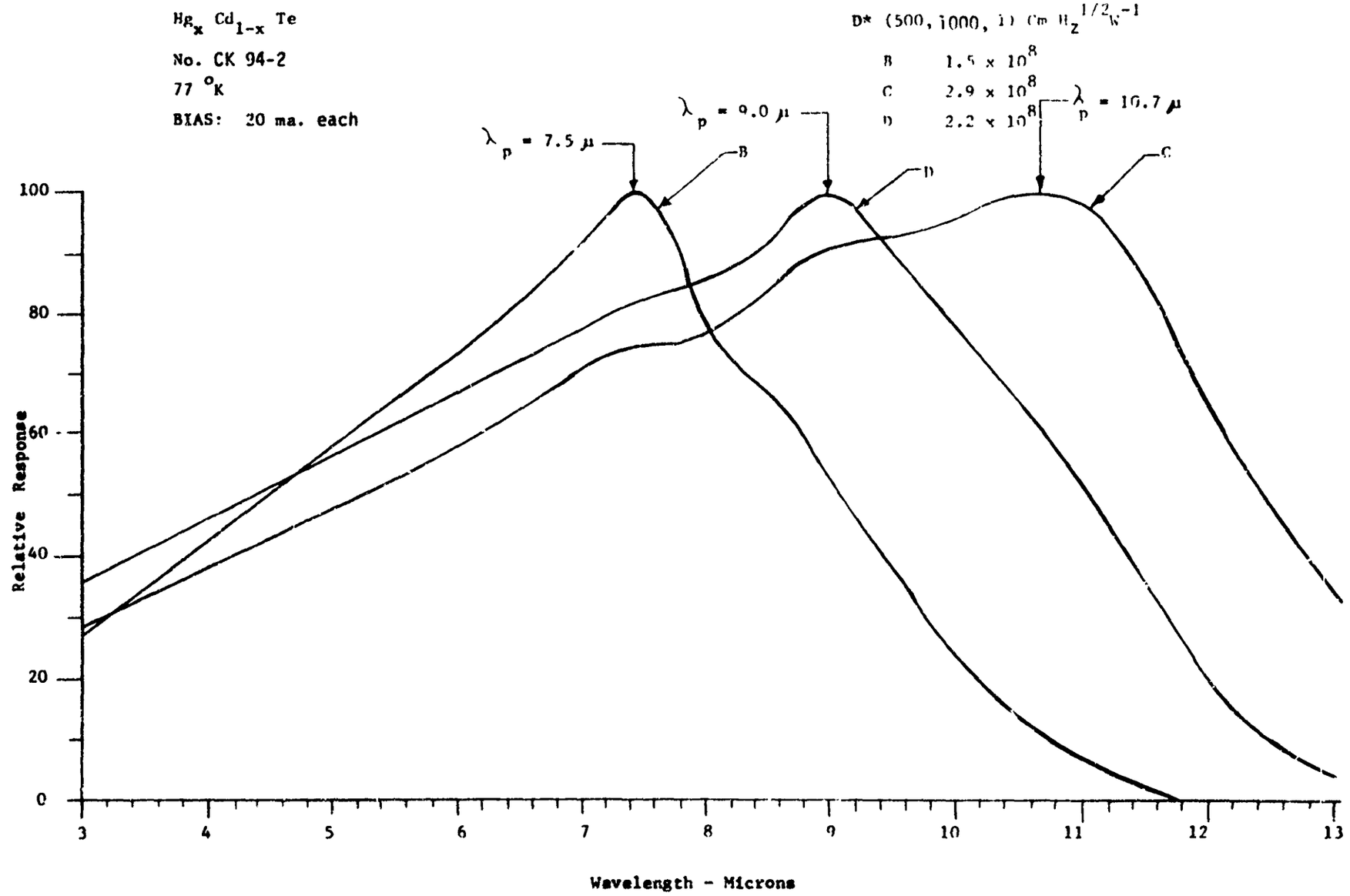
$Hg_x\ Cd_{1-x}\ Te$
No. CK 94-2
77 °K
BIAS: 20 ma. each
D* (500, 1000, 1) Cm $Hz^{1/2}W^{-1}$
B 1.5 x 10^8
C 2.9 x 10^8
D 2.2 x 10^8
λ_p = 7.5 μ
λ_p = 9.0 μ
λ_p = 10.7 μ
B
D
C
Relative Response
100
80
60
40
20
0
3
4
5
6
7
8
9
10
11
12
13
Wavelength - Microns

Figure 6-2

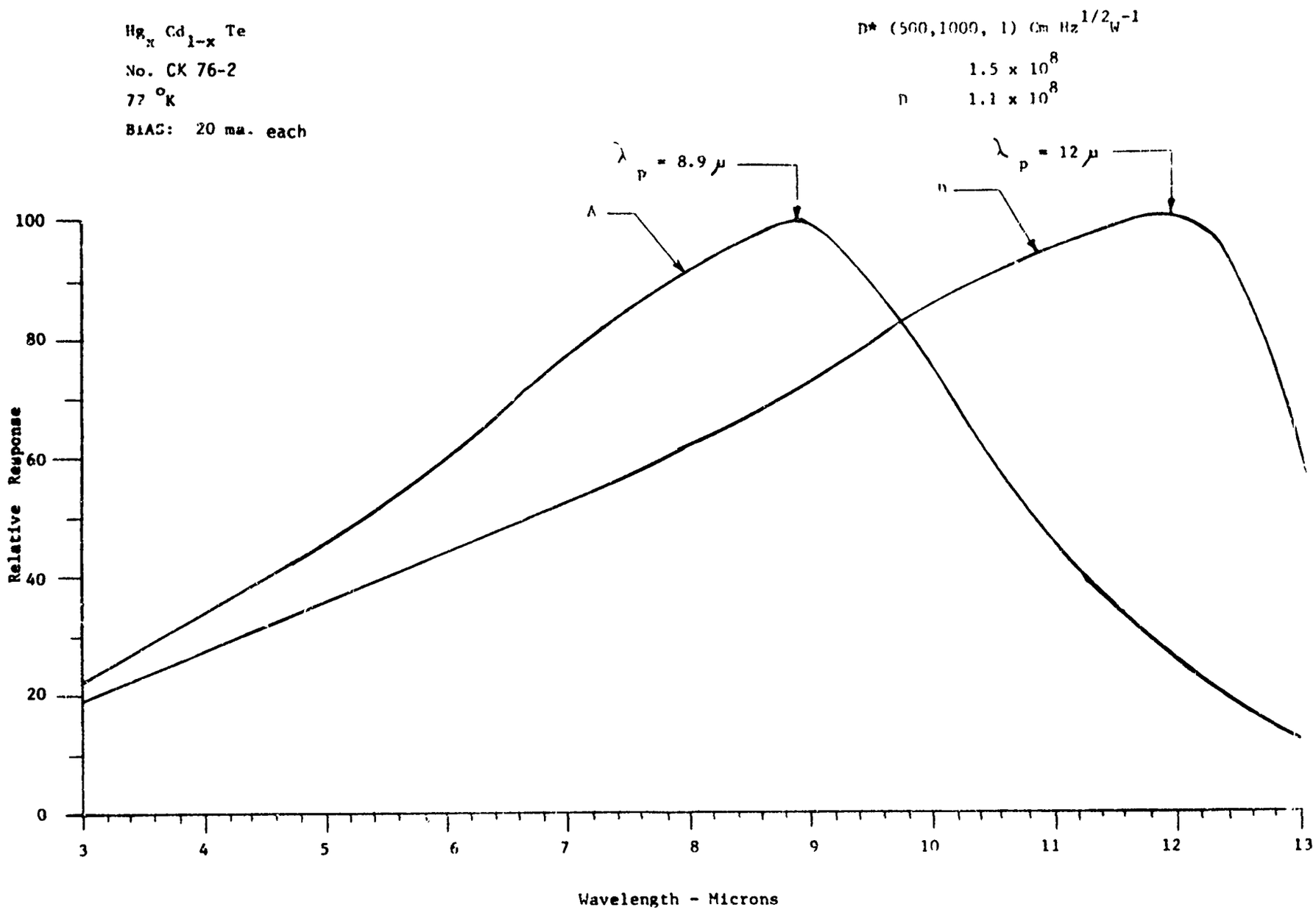
$Hg_x Cd_{1-x} Te$
No. CK 76-2
77 °K
BIAS: 20 ma. each
D* (500,1000, 1) Cm $Hz^{1/2}W^{-1}$
1.5×10^8
n 1.1×10^8
$\lambda_p = 8.9\mu$
$\lambda_p = 12\mu$
A
n
100
80
60
40
20
0
Relative Response
3
4
5
6
7
8
9
10
11
12
13
Wavelength - Microns

Figure 6-3

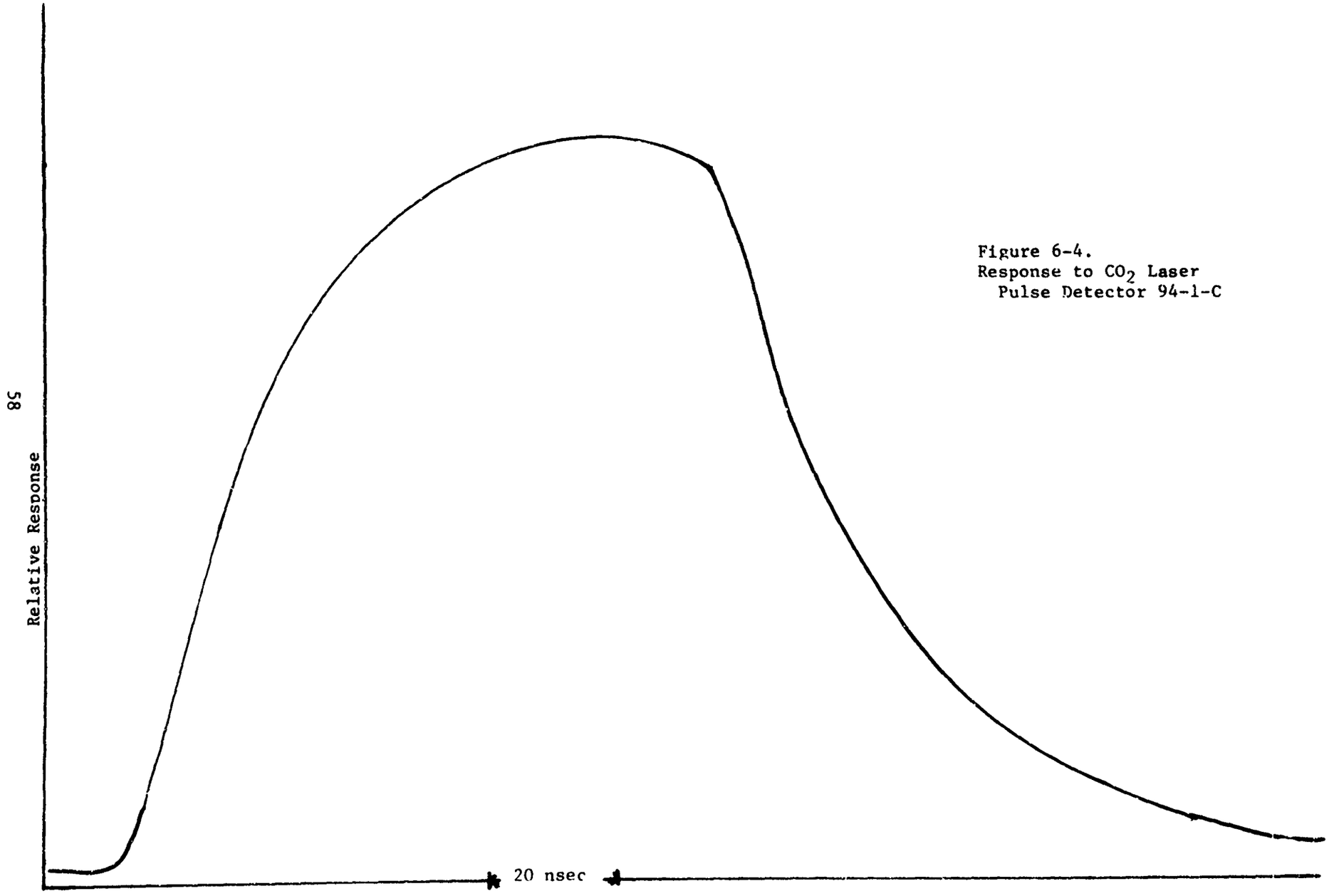

Figure 6-4.
Response to CO_2 Laser
Pulse Detector 94-1-C

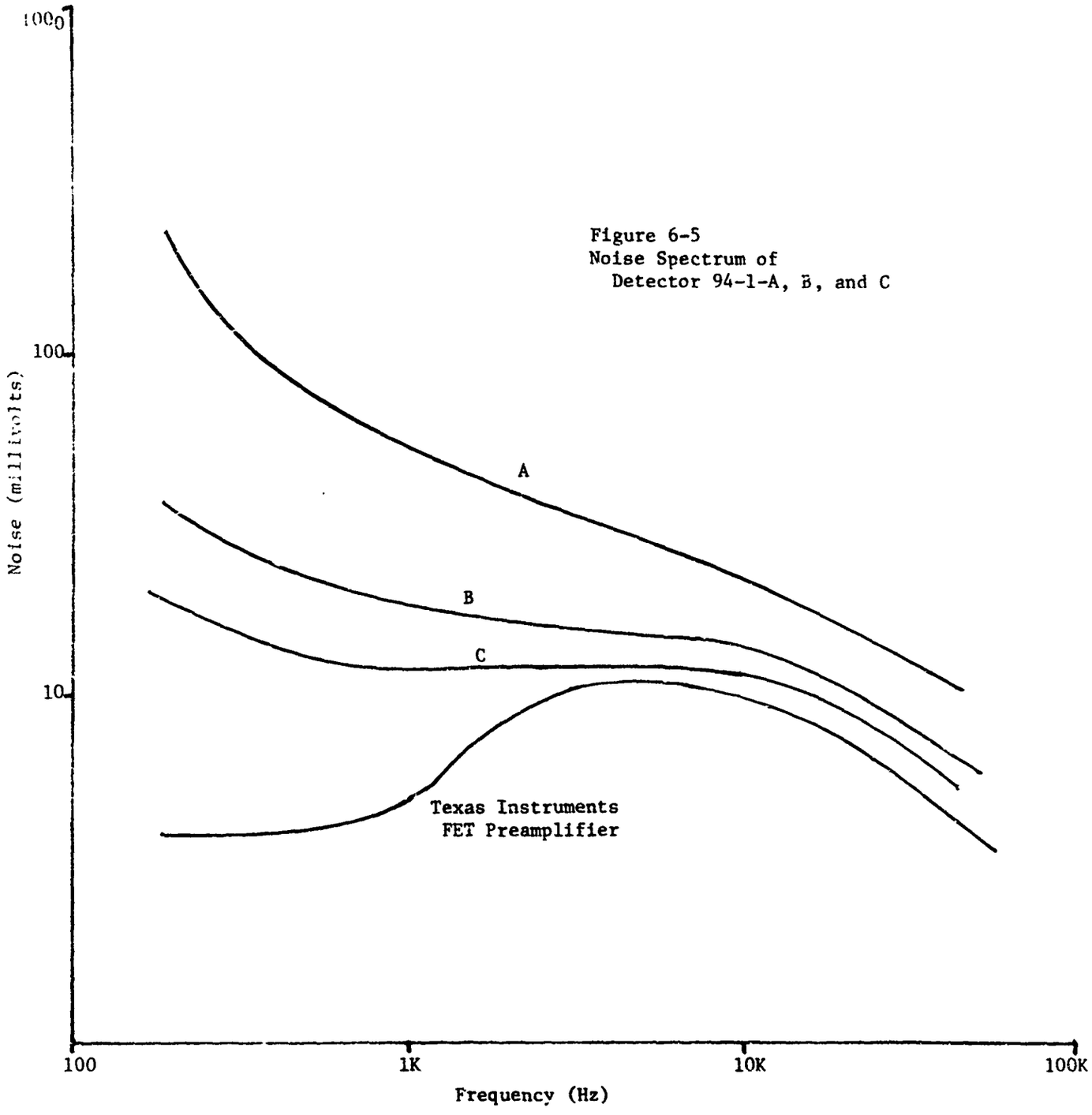

Figure 6-5
Noise Spectrum of
Detector 94-1-A, B, and C

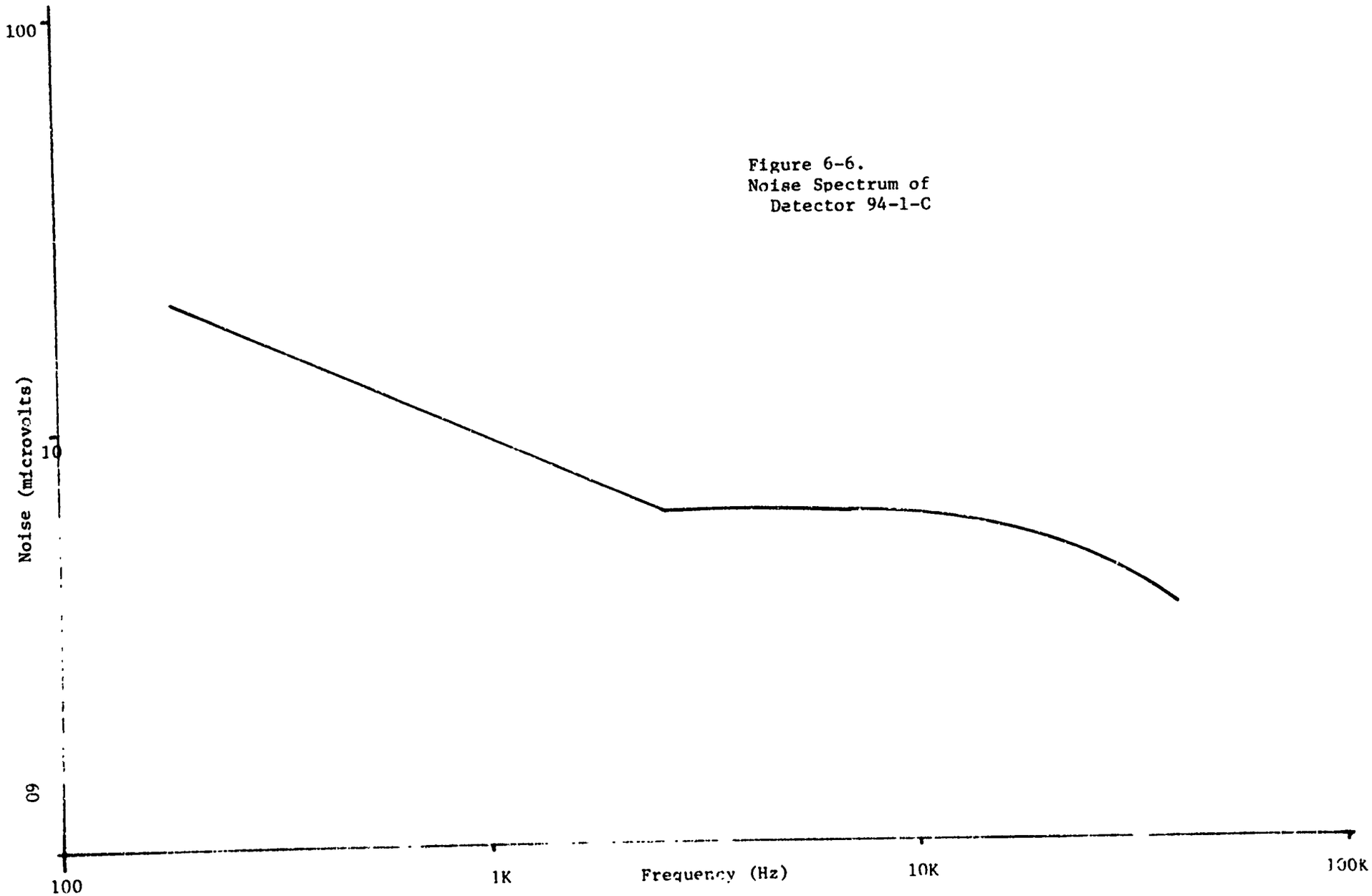

Figure 6-6.
Noise Spectrum of
Detector 94-1-C

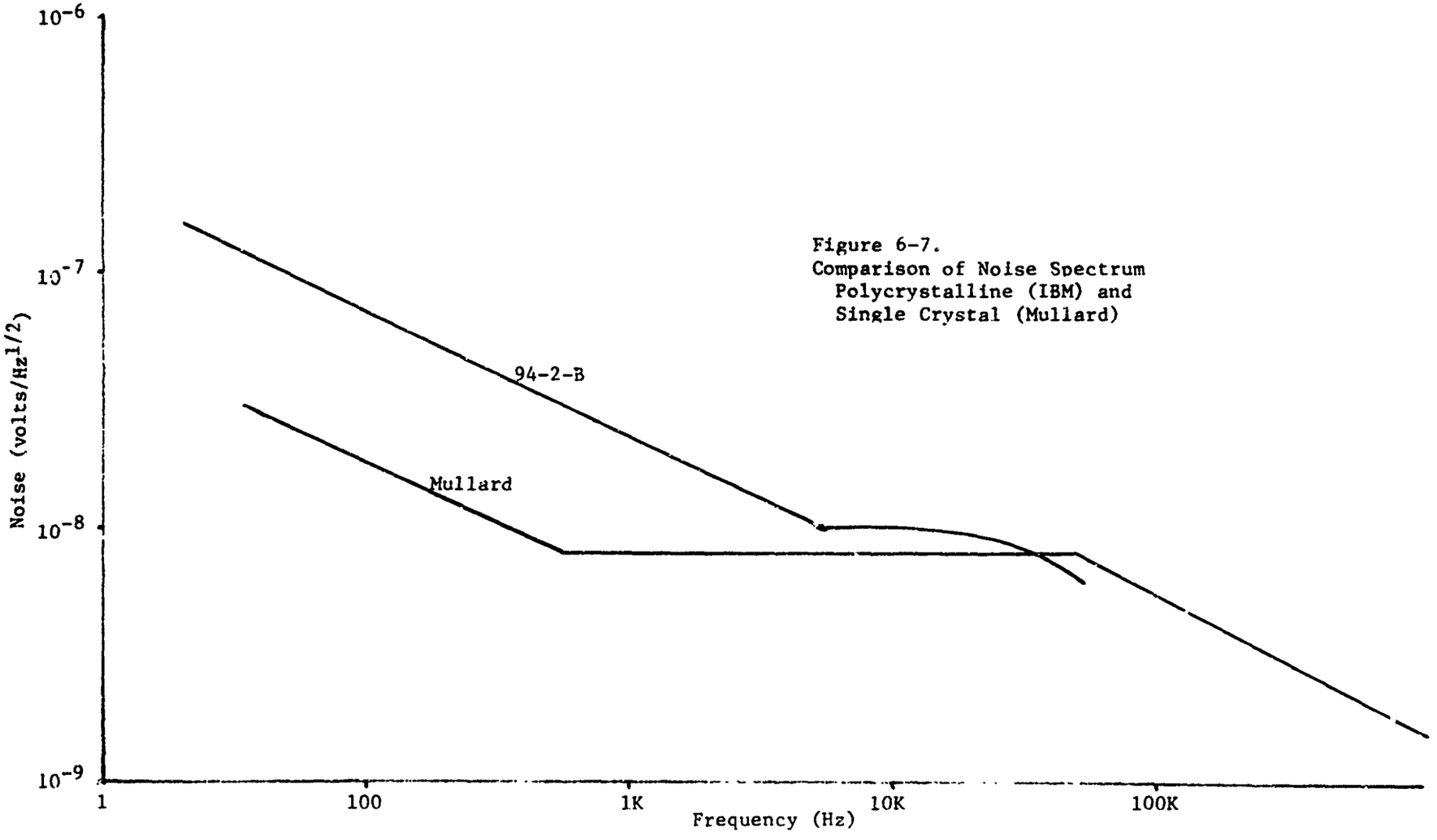

Figure 6-7.
Comparison of Noise Spectrum
Polycrystalline (IBM) and
Single Crystal (Mullard)

Section 7

NEUTRON IRRADIATION OF HgCdTe INFRARED DETECTORS

A single three-element array (area: 2×10^{-1} cm^2) HgCdTe IR photodetector (#251A) was subjected to 8.7×10^{13} neutrons/cm^2 at the White Sands Fast Burst Reactor. The devices irradiated were epitaxially grown, polycrystalline HgCdTe sensors fabricated by IBM. To avoid instantaneous temperature rises associated with the fast burst mode of operation, the reactor was run in a power mode with the above dose accumulated over a period of steady irradiations lasting about three hours.

Pre- and post-test measurements of resistance, D*, and signal and noise increase factor were made at the IBM Owego facility. The results of these measurements are summarized in the following table. Caution should be used in interpreting the data since controls were not employed and the detector's parameters were subject to some drift.

Table 7-1
Results of Neutron Irradiation

	D* (500°K, 1000 Hz, 1) $CmHz^{1/2}\omega^{-1}$		
Element	1-2	2-3	3-4
Before Test	2.9×10^8	1.6×10^8	1.3×10^8
After Test	4.0×10^7	4.0×10^7	2.9×10^8
D* Reduction (Factor)	7	4	4

Signal and Noise Increase Factor
(after irradiation)

Signal	2 - 3	2 - 3	(decrease of 2)
Noise	13 - 20	11 - 12	1 - 3

Resistance

	$R_{300°K}$ - ohms		$R_{77°K}$ - ohms	
Element	Before	After*	Before	After*
1-2	4.0K	6.3K	300K	1M
2-3	7.3K	2.5K	46K	4.1K
3-4	15K	13K	400K	800K

* New indium contacts to detector elements.

On the basis of one sample, a reduction in D* by a factor of 4 to 7 was observed after nuclear bombardment of the three element HgCdTe detector. Although the S/N ratio after the test was less than before (and thus a smaller D*), an analysis of the signal and noise showed that for two detector elements the signal increased by a factor of 2 to 3 while the noise in the same elements also increased by a factor of 11 to 20. The third element showed a decrease in signal (by a factor of 1.5 to 2) and an increase of noise of about 3.

The original indium contacts to the gold stripes on the detector came off when the detectors were cooled to 77°K. New contacts were then made which easily withstood the temperature cycle. Because of the change in contacts, it is difficult to analyze the resistance data meaningfully. However, the new contacts should not have impacted D* or signal and noise measurements.

An apparent shift in spectral sensitivity was also observed. The vycor filter percent cutoff increased from 5 - 10 percent to 24 - 28 percent. The sapphire percent cutoff decreased from 5 - 10 percent to 0 percent. Apparently, the neutron irradiation produced a λ_p shift to shorter wavelength (possible loss of mercury).

Although the polycrystalline HgCdTe detector irradiated showed appreciable degradation, sufficient D* remained to consider the detector a usable device for many applications. The polycrystalline device should be less sensitive to neutron damage than single crystal detector having equivalent sensitivity. It is suggested that a more thorough test and a more thorough pre/post sample characterization be performed to better evaluate this type of detector.

Also, transient measurements at a pulse flash x-ray facility are desirable to establish malfunction levels. These tests should be directed not only toward characterizing the detector in irradiation environment but also toward understanding the basic mechanisms involved with the view of possibly identifying minor process changes which could considerably enhance the hardness of the detector.

Section 8

SUMMARY

Vapor absorption measurements were performed on the elements mercury, cadmium, and tellurium in both static cells and in the flowing gas (dynamic) open tube growth system. The results indicate that the dynamic system, under specific operating conditions, can demonstrate the same dependency relationship between source temperature and resultant optical density of the source vapor as was obtained in a closed, static system.

To obtain better control of the cold finger temperature, a balanced-radiation apparatus was designed and fabricated. In simulated crystal growing experiments, this device exhibits a very small radial temperature gradient.

Hall measurements have been made on both "as grown" and annealed samples. It was observed that the Hall coefficient is a strong function of the mercury. Results of these measurements indicate that the carrier concentration can be minimized by the correct mercury pressure during the annealing process.

In regard to crystal growth, a considerable number of growth runs were made to determine the effect of a cold finger pedestal temperature change and of growth times upon the resulting growths. Both the relative percent (by x-ray fluorescence) mercury, cadmium, and tellurium were monitored as well as the total growth thickness and percentage sapphire cutoff. It was determined that the best detectors were produced in the temperature range of 594°C to 602°C for the chosen values of mercury, cadmium, and tellurium source temperatures. In addition, adequate data were taken to establish statistical ranges, indicating the reliability of results. It was also shown that the growth time had little effect on the quality of the detectors produced but increased growth times did produce larger crystallites and an indicated lower percentage of mercury. However, good detectors were produced with growth times as short as one-quarter hour and as long as eight hours.

Unclassified

Security Classification

DOCUMENT CONTROL DATA - R & D

(Security classification of title, body of abstract and indexing annotation must be entered when the overall report is classified)

1 ORIGINATING ACTIVITY *(Corporate author)*
IBM Corporation
Federal Systems Division, Electronics Systems Ctr
Owego, New York 13827

2a. REPORT SECURITY CLASSIFICATION
Unclassified

2b. GROUP

3 REPORT TITLE

Epitaxial Vapor Growth of $Hg_{1-x}Cd_xTe$ in an Open-Tube Apparatus

4 DESCRIPTIVE NOTES *(Type of report and inclusive dates)*
Final Report, 2-1-69 through 2-1-70

5 AUTHOR(S) *(First name, middle initial, last name)*
Donald R. Carpenter Arthur T. Halpin
Robert M. Kloepper Paul B. Pickar

6 REPORT DATE	7a. TOTAL NO. OF PAGES	7b. NO. OF REFS
March, 1970	70	0

8a. CONTRACT OR GRANT NO.	9a. ORIGINATOR'S REPORT NUMBER(S)
N00019-69-C-0398	70-M46-03
b. PROJECT NO.	
c.	9b. OTHER REPORT NO(S) *(Any other numbers that may be assigned this report)*
d.	

10 DISTRIBUTION STATEMENT

11. SUPPLEMENTARY NOTES

12. SPONSORING MILITARY ACTIVITY
Naval Air Systems Command
Department of the Navy
Washington, D. C.

13 ABSTRACT

Vapor absorption measurements were performed on the elements mercury, cadmium, and tellurium in both static cells and in the flowing gas (dynamic) open tube growth system. The results indicate that the dynamic system, under specific operating conditions, can demonstrate the same dependency relationship between source temperature and resultant optical density of the source vapor as was obtained in a closed, static system.

To obtain better control of the cold finger temperature, a balanced radiation apparatus was designed and fabricated. In simulated crystal growing experiments, this device exhibits a very small radial temperature gradient. Hall measurements have been made on both "as grown" and annealed samples.

In regard to crystal growth, a considerable number of growth runs were made to determine the effect of a cold finger pedestal temperature change and of growth times upon the resulting growth. It was observed that the best detectors were produced in the temperature range (substrate temperature) of 594° to 602°C for the chosen values of mercury, cadmium, and tellurium source temperatures. Experimental infrared detectors have been fabricated exhibiting D* values in the region of 10^9cm $Hz^{1/2}w^{-1}$, with peak in the region of 10 microns.

DD FORM 1 NOV 68 1473 REPLACES DD FORM 1473, 1 JAN 64, WHICH IS OBSOLETE FOR ARMY USE.

Security Classification

Security Classification

14. KEY WORDS	LINK A		LINK B		LINK C	
	ROLE	WT	ROLE	WT	ROLE	WT
Epitaxial Growth						
Epitaxy						
Infrared Radiation Detector						
Mercury-Cadmium-Telluride Growth						
Photoconductive Devices						